CHEMISTRY
A EUROPEAN JOURNAL

DOI: 10.1002/chem.200601708

Allyl *ansa*-Lanthanidocenes: Single-Component, Single-Site Catalysts for Controlled Syndiospecific Styrene and Styrene–Ethylene (Co)Polymerization

Anne-Sophie Rodrigues,[a] Evgueni Kirillov,[a] Christian W. Lehmann,[b] Thierry Roisnel,[c] Bruno Vuillemin,[d] Abbas Razavi,[e] and Jean-François Carpentier*[a]

Abstract: A series of new neutral allyl Group 3 metal complexes bearing *ansa*-bridged fluorenyl/cyclopentadienyl ligands [{Flu-EMe$_2$-(3-R-Cp)}Ln(η^3-C$_3$H$_5$)(THF)] (E = C, R = H, Ln = Y (**2**), La (**3**), Nd (**4**), Sm (**5**); R = *t*Bu, Ln = Y (**8**), Nd (**9**); E = Si, R = H, Ln = Y (**12**), Nd (**13**)) were synthesized in good yields via salt metathesis protocols. The complexes were characterized by elemental analysis, NMR spectroscopy for diamagnetic complexes, and single-crystal X-ray diffraction studies for **2**, **4**, **9** and **12**. Some of the allyl *ansa*-lanthanidocenes, especially **4**, are effective single-component catalysts for the polymerization of styrene, giving pure syndiotactic polystyrenes (*rrrr* > 99%) with low to high molecular weights (M_n = 6000–135000 g mol^{-1}) and narrow polydispersities (M_w/M_n = 1.2–2.6). The catalyst systems are remarkably stable, capable of polymerizing styrene up to 120 °C with high activities, while maintaining high syndiotacticity via chain-end control as established by a Bernoullian analysis. Highly effective copolymerization of styrene with ethylene was achieved using neodymium complex **4** (activity up to 2530 kg PS-PE mol^{-1} h^{-1}) to give true copolymers void of homopolymers with M_n = 9000–152000 g mol^{-1} and narrow polydispersities (M_w/M_n = 1.2–2.5). The nature of the resultant P(S-*co*-E) copolymers was ascertained by NMR, size-exclusion chromatography/refractive index/UV, temperature rising elusion fractionation, and differential scanning calorimetry. It is shown that, regardless the amount of ethylene incorporated (1–50 mol%), P(S-*co*-E) copolymers have a microstructure predominantly made of long highly syndiotactic PS sequences separated by single or few ethylene units. Co-monomers feed and polymerization temperature can be used straightforwardly to manipulate with the physical and mechanical characteristics of the P(S-*co*-E) copolymers (molecular weights and distributions, co-monomer content, microstructure, T_m, T_g, T_c).

Keywords: allyl complexes · copolymers · lanthanide · polymerization · styrene

Introduction

Processes for the production of polyolefins with controlled microstructure and (pre)requisite properties are at the forefront of industrial polymerization technology.[1] Central to this field is the design and development of efficient, well-defined "single-site" polymerization catalytic systems. Syndiospecific (co)polymerization of styrenic monomers constitutes a relevant example of a technology-driven process for the production of commercial materials with valuable properties for myriad applications.[2] Highly syndiotactic polystyrene (sPS), originally disclosed by Ishihara at Idemitsu,[2,3] is available via conventional Ziegler–Natta catalysis using a variety of precursors incorporating transition metals, mostly Ti. Among the most active catalysts, which afford sPS with high contents of racemic *pentads* (*rrrr* > 90%), are the homogeneous two-component mono-cyclopentadienyl systems (represented by the general type **A**, see below), where the π-coordinated donor can be any of cyclopentadienyl-related ligands, for example, indenyl, fluorenyl.[2,4] Since the open-

[a] Dipl.-Ing. Chem. A.-S. Rodrigues, Dr. E. Kirillov, Prof. Dr. J.-F. Carpentier
Sciences Chimiques de Rennes
UMR 6226 CNRS-Université de Rennes 1
35042 Rennes Cedex (France)
Fax: (+33) 223-236-939
E-mail: jean-francois.carpentier@univ-rennes1.fr

[b] Dr. C. W. Lehmann
Max-Planck-Institut für Kohlenforschung
Chemical Crystallography
Postfach 101353, 45466 Mülheim/Ruhr (Germany)

[c] Dr. T. Roisnel
Centre de Diffractométrie X, Université de Rennes 1
35042 Rennes Cedex (France)

[d] Dr. B. Vuillemin
Total Petrochemicals
64170 Mont-Lacq (France)

[e] Dr. A. Razavi
Total Petrochemicals Research
Zone Industrielle C, 7181 Feluy (Belgium)

Supporting information for this article is available on the WWW under http://www.chemeurj.org/ or from the author: Spectral data for all diamagnetic complexes and polymer analytical data.

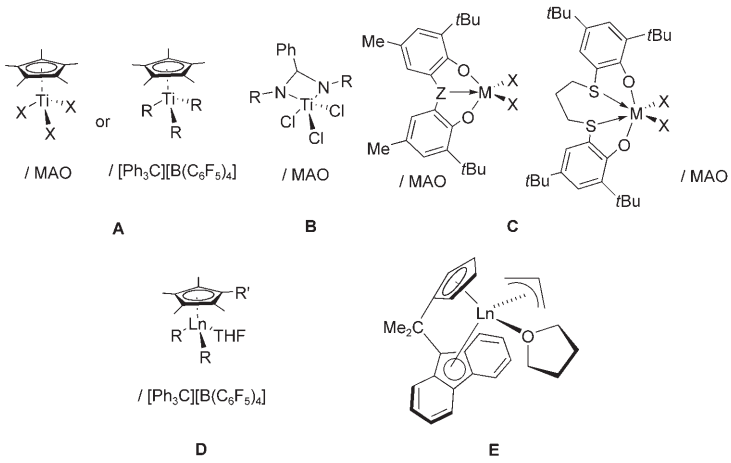

ing of the post-metallocene polymerization catalysis era, several cyclopentadienyl-free systems enabling controlled syndiospecific polymerization of styrene have emerged. For example, sPS production using amidinate precursors (type **B**) was reported by Rausch[5] and Zambelli.[6] Recently, Okuda reported series of Ti- and Zr-based precursors with sulfur-bridged bis(phenolate) ligands (type **C**) capable of efficiently polymerizing styrene in a syndiospecific manner.[7] In fact, it appears that any Group 4 metal precursor prone to generate under the polymerization conditions the generally accepted "true" active species $[(L)M^{III}\text{-}R]^+$ (where L is a ligand, and R an alkyl group) may promote syndiospecific polymerization of styrene.[2] Recent investigations by Hou[8] and by Okuda[9] have exemplified that highly stereoregular sPS can also be obtained using Group 3 half-metallocene cationic precursors (type **D**), which are isovalent and isostructural to the afore mentioned Group 4 metal alkyl cation.

Besides all its desirable properties (e.g., high crystallization rate, low specific gravity and dielectric constant, high modulus of elasticity, excellent chemical resistance), sPS possesses properties, which constitute major limitations from an industrial/processing point of view, that is, brittleness and high melting temperature (ca. 260–270 °C). An important method for modifying properties of this polymer is the incorporation of ethylene (or an α-olefin) using common copolymerization protocol. For instance, the ethylene–styrene interpolymers (ESI) with low styrene incorporation are crystalline thermoplastic materials, whereas those with relatively high degree of styrene units (>50 mol %) pseudo-randomly enchained feature amorphous elastomeric properties and are therefore so-called "glasstomers".[10] Taking into account the dissimilar nature of the species responsible for stereospecific incorporation of styrene and ethylene enchainment, the efficient and stereoselective copolymerization of these two monomers has remained an arduous but challenging task. Many of the traditional catalytic systems capable of producing sPS have been assessed in copolymerization of styrene with ethylene, however, usually affording atactic or alternating structures, scarce performances and/or often mixtures of homopolymers.[11,12] Therefore, enormous endeavours have been made to expand on the polymerization systems and strategies to bring a substantial control for the rational engineering of such polymeric materials. Nevertheless, successful examples still remain rare. Among those remarkable achievements, Marks' dinuclear CGC–titanium system copolymerizes very efficiently styrene and ethylene, however, giving random copolymers with atactic PS sequences.[13] Living copolymerization of ethylene with styrene to give styrene-poor (<32 mol %) copolymers using the Cp*Ti(=NR)Cl_2/MAO binary system was recently reported.[14] The unprecedented ability of some Group 3 metal complexes to afford high control in the copolymerization of styrene and ethylene was shown by Hou.[8] These bicomponent cationic systems (such as **D**, see above) are capable of producing P(S-*co*-E) copolymers with a high styrene content (13–87 mol %) and a remarkable microstructure where highly syndiotactic PS sequences are merged with PE blocks in an alternating manner.

Recently, we reported the highly syndiospecific polymerization of styrene mediated by a new family of single-component, single-site organolanthanide catalysts, that is, neutral allyl complexes supported by the *ansa*-bridged cyclopentadienyl/fluorenyl ligand $[Cp\text{-}CMe_2\text{-}Flu]^{2-}$ (**E**, see above).[15] Allyl complexes of Group 3 metals have been known since the pioneering work of Tsutsui.[16] Posterior essential contributions on their synthesis and structure have been made by Schumann and Marks,[17] Evans,[18] Bercaw,[19] Bochmann,[20] and others.[21] However, only in a few cases, the polymerization catalytic performances of allyl–lanthanide complexes were explored.[22] In this contribution, we describe a general synthetic approach via simple salt metathesis protocols of Group 3 neutral allyl complexes based on different $[Flu\text{-}EMe_2\text{-}(3\text{-}R\text{-}Cp)]^{2-}$ ligands (E = C, Si and R = H, *t*Bu) and discuss their structural features in the solid state and in solution. It is shown that some of these precursors are highly competent for the syndiospecific homopolymerization of styrene and its copolymerization with ethylene to afford microstructurally controlled P(S-*co*-E) materials with very high styrene content and advanced characteristics. The central aim of this work was to establish structure–catalytic performance relationships and bring together the complete picture of this new single-component coordinative/insertive polymerization promoted by neutral allyl complexes of lanthanides.

Results

Generalized approach towards neutral allyl *ansa*-lanthanidocenes [{Flu-EMe_2-(3-R-Cp)}Ln(C_3H_4)(THF)] (E = C, Si; R = H, *t*Bu; R′ = H, Me; Ln = Y, La, Nd, Sm): Previous work in our group has shown that reaction of the anionic complex $[(Cp\text{-}CMe_2\text{-}Flu)YCl_2]^-[Li(ether)_4]^+$ (ether = Et_2O, THF) (**1**)[23] with lithium reagents offers a facile and efficient entry towards neutral yttrium carbyl and hydrido derivatives [{Cp-CMe_2-Flu}YR(THF)] (R = $CH(SiMe_3)_2$,

CH_2SiMe_3, H).[24] Similarly, the salt metathesis reaction of **1** with the Grignard reagent [$ClMg(C_3H_5)$] (1 equiv vs Y, as a THF solution) in toluene at 20°C gives the neutral allyl complex [{Flu-CMe_2-Cp}$Y(C_3H_5)$(THF)] (**2**) as a yellow microcrystalline powder in 65% isolated yield [Scheme 1, Eq. (1)].[15,25] The parent complexes of La (**3**), Nd (**4**) and Sm (**5**) were obtained analogously in good yields using a one-pot procedure employing first the reaction of the dilithium salt of the [Flu-CMe_2-Cp] ligand with $LnCl_3$·THF adducts, followed by allylation of the crude products formed with the allyl Grignard reagent (see Experimental Section for details).

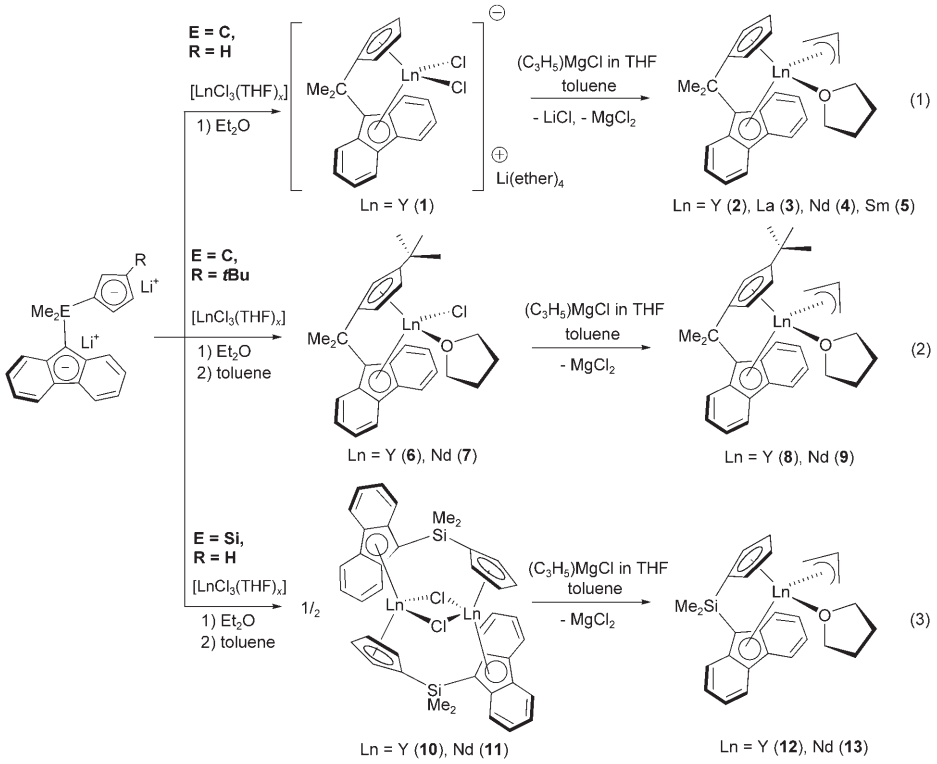

Scheme 1. Synthetic routes towards neutral allyl *ansa*-lanthanidocenes supported by fluorenyl/cyclopentadienyl ligands; ether: THF, Et_2O.

In general, substituted *ansa*-bis(cyclopentadienyl) systems are known to form stable solvent-free, electron-poor alkyl complexes with rare-earth metals.[26] Conversely, the mono-THF adducts of allyl complexes **8** and **9** were obtained when using the corresponding *t*Bu-substituted cyclopentadienyl ligand [Scheme 1, Eq. (2)]. As a matter of fact, the transmetallation reaction of the dilithium salt of this ligand with $[YCl_3(THF)_{3.5}]$ affords neutral [{(3-*t*Bu-C_5H_3)-CMe_2-Flu}YCl(THF)] (**6**) which then reacts with 1 equiv of allyl Grignard reagent in toluene to give **8** in 69% isolated yield. The neodymium analogue was obtained similarly in 54% yield.

To explore the possible impact of the bite angle Cp_{cent}-XR_2-Flu_{cent} on catalytic performance,[1a,27] we were interested in obtaining also silylene-bridged instead of isopropylidene-bridged complexes. Qian and co-workers have reported that the reaction between [Flu-$SiMe_2$-Cp]Li_2 and YCl_3 results in the isolation of base-free dinuclear complex **10**, which features a "spanned" coordination of the Me_2Si-bridged ligand.[28] Following this procedure, yttrium complex **10** and its new neodymium analogue **11** were prepared and further reacted with 1 equiv of allyl Grignard reagent to afford the corresponding neutral allyl complexes **12** and **13** in 60 and 76% isolated yields, respectively [Scheme 1, Eq. (3)].

Complexes **2**–**5**, **12** and **13** are insoluble in aliphatic hydrocarbons (pentane, hexane), fairly soluble in toluene, while complexes **8** and **9** that bear a *t*Bu-substituted fluorenyl moiety feature enhanced solubility in aromatic hydrocarbons. Rapid substantial decomposition of **2**, **3** and **8** in THF solution at room temperature was indicated by ^{1}H NMR spectroscopy to give unidentified products.

Recently, Evans reported that various [$Cp'_2Y(C_3H_5)$(THF)] complexes ($Cp' =$ substituted Cp ligands) readily eliminate the coordinated THF molecule upon moderate heating under vacuum, affording base-free species.[18c] Notwithstanding, no perceptible abstraction of THF in complexes **2**, **4**, **8**, **9** and **12** was observed, even upon prolonged heating at 60°C under dynamic vacuum.[29]

Molecular structure of allyl complexes 2, 4, 9 and 12: Single crystals of allyl complexes **2**, **4**, **9** and **12** suitable for X-ray crystallography were grown at room temperature from diluted toluene solutions. The solid-state molecular structures of **4**, **9** and **12** are shown in Figures 1–3 and selected geometrical parameters (bond lengths and angles) are given in Table 1.[30] All the allyl complexes synthesized are mono-THF adducts and adopt a pseudo-tetrahedral coordination sphere about the metal centers, similar to that found in a large variety of complexes of general formula [Cp_2LnXX'].[31] Considering the similarity of the M–C11–C15 bond lengths, the cyclopentadienyl moiety is η^5-bonded to the metal center in all three complexes. The M–C(Cp) bond lengths in **4** and **9** (2.696(10)–2.863(5) Å) are longer than those described in closely related neodymium complexes (2.691(5)–2.771(4) Å),[32] whereas those in **12** (2.6215(19)–2.7109(18) Å) fall in the normal range of M–C(Cp) bond lengths found in parent yttrium complexes (2.56(2)–2.790(4) Å).[28,33] On the other hand, the fluorenyl

moiety in **4**, **9** and **12** clearly features an η^3-bonding mode by the central five-membered ring, as evidenced from the M−C(Flu) bond lengths: in all three complexes, the bond lengths involving the bridgehead and the two adjacent carbon atoms M−C9, M−C9a, and M−C8a are significantly shorter than the two distal ones M−C4a and M−C4b. The average values of 2.754(9) and 2.768(9) Å for Nd−C(9,8a,9a) bond lengths in **4** and **9**, respectively, compare well with those of congener neodymium complexes bearing a Ph_2C-bridged fluorenyl/cyclopentadienyl ligand (2.774(5)–2.783(5) Å).[32] The corresponding value for **12** (2.713(2) Å) is slightly greater than those described for related yttrium complexes incorporating Me_2Si-bridged fluorenyl/cyclopentadienyl ligand (2.653(4)–2.674(4) Å).[28,33] Complexes **4** and **9** incorporating the isopropylidene-bridged ligand feature very narrow bite angles Cp_{cent}-Nd-Flu_{cent} of 93.88(5) and 93.87(14)°, respectively, which are about 10° lower than in known [Flu-CR_2-Cp]LnX of early lanthanides,[23,24] and constitute a unique feature of these complexes. As expected, the larger bite angle of 106.28° in **12** is in agreement with the longer linking Me_2Si-spacer unit.[27] The allyl fragment in **4**, **9** and **12**[34] is coordinated in an η^3-mode, though in a rather non-symmetric manner, as judged by the about 0.1–0.2 Å difference in the M−C(allyl) distances, especially in **9**; also, the C−C bonds in the allyl ligands are far from being equal. This peculiarity could arise from either severe steric congestion induced by the neighboring coordinated THF molecule and/or non-equal participation of the sp^2-carbon atoms in bonding with the metal center. The M−C(allyl) bond lengths in **4**, **9** and **12** are somewhat longer than the usual range for Nd−allyl (2.699(9)–2.786(9) Å)[21b–e] and Y−allyl (2.545(5)–2.613(3) Å) complexes.[18c] Considering an η^3-coordination mode for both the allyl fragment and fluorenyl ligand, the eight-coordinate allyl complexes **2**, **4**, **9** and **12** can be considered as formal 16-electron species.

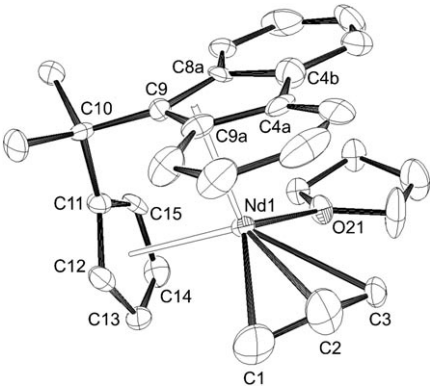

Figure 1. Crystal structure of [(Flu-CMe_2-Cp)Nd(C_3H_5)(THF)] (**4**).

Variable-temperature (VT) NMR investigations: The solution structures of the diamagnetic allyl complexes **2**, **3**[35] and **12** were studied by variable temperature ^{1}H NMR spectroscopy.[36] In [D_8]toluene solution, the allyl complexes feature

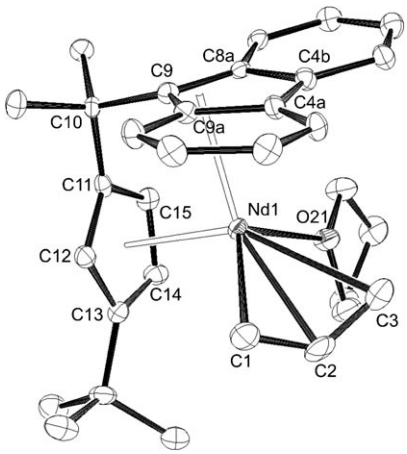

Figure 2. Crystal structure of [(Flu-CMe_2-(3-*t*Bu-Cp))Nd(C_3H_5)(THF)] (**9**).

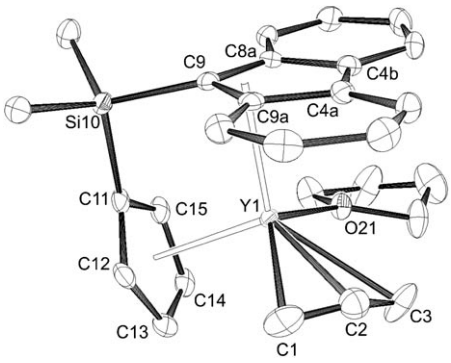

Figure 3. Molecular structure of [(Flu-$SiMe_2$-Cp)Y(C_3H_5)(THF)] (**12**) (second disordered methine carbon atom C2′ is omitted for clarity).

Table 1. Selected bond lengths [Å] and angles [°] for complexes **4**, **9** and **12**.

	4	**9**	**12**
M−C1	2.656(12)	2.639(5)	2.583(2)
M−C2	2.700(11)	2.756(5)	2.571(10) (2.607(3))[a]
M−C3	2.725(9)	2.818(5)	2.649(2)
M−C4a	2.982(10)	2.949(5)	2.978(2)
M−C4b	2.935(10)	2.927(5)	2.922(2)
M−C8a	2.767(10)	2.779(4)	2.7109(18)
M−C9a	2.825(10)	2.843(5)	2.8002(16)
M−C9	2.673(8)	2.682(5)	2.627(2)
M−Flu_{cent}	2.559(9)	2.573(5)	2.513(8)
M−C11	2.695(9)	2.658(4)	2.6215(19)
M−C12	2.697(10)	2.729(5)	2.6249(19)
M−C13	2.766(10)	2.863(5)	2.688(2)
M−C14	2.806(10)	2.823(5)	2.693(2)
M−C15	2.757(9)	2.685(5)	2.6281(17)
M−Cp_{cent}	2.464(9)	2.472(5)	2.363(8)
M−O21	2.494(7)	2.470(3)	2.4519(14)
Cp_{cent}-M-Flu_{cent}	93.88(5)	93.87(14)	106.28(7)
C1−C2	1.287(18)	1.407(7)	1.160(10) (1.360(4))[a]
C2−C3	1.31(2)	1.377(7)	1.449(11) (1.374(4))[a]

[a] Bond with the disordered methine C2′ atom.

all a dynamic behavior. At 298 K, complexes **2** and **12** appear symmetric on the NMR time scale exhibiting four ^{1}H NMR resonances for the Flu group, two resonances for the Cp group and one resonance for the Me_2E bridge (Figure 4). Interestingly, the allyl moiety is presented solely by two signals (AX_4 splitting pattern), that is, a quintet from the methine proton and a doublet from both *anti* and *syn* protons (Table 2). This fact can be rationalized considering the allyl ligand in rapid motion (on the NMR time scale),[37] which can occur via two possible mechanisms scrutinized by Bercaw et al. for base-free allyl-scandocene complexes: i) 180° rotation of the η^3-allyl moiety, and ii) $\eta^3 \leftrightarrow \eta^1$ isomerization/interconversion.[19] As the temperature is decreased, a substantial broadening of most of the signals is first observed and the fluxional process is frozen out below 223 K (Figure 4). The ^{1}H NMR spectra at 203 K of **2** and **12** each display sets of relatively sharp resonances consistent with a dissymmetric structure, which include eight resonances for the Flu groups, four resonances for the Cp groups and two resonances for the Me_2E bridge. Five resonances are observed for the allyl protons, with a characteristic AGMPX pattern.[19] These observations are consistent with at least three independent dynamic processes, which may eventually be concomitant: i) allyl η^3 rotation and ii) $\eta^3 \leftrightarrow \eta^1$ isomerization, as already mentioned, and iii) THF dissociation.[38] One can not discard also that a fluxional behavior associated with hapticity rearrangements of the π-bonded fluorenyl ligand might operate as well.[27] However, in contrast with fluorenyl complexes of late transition metals,[39] no reversible haptotropic rearrangements have been clearly documented for early transition-metal complexes so far.[27a,40] Thus, VT ^{1}H NMR spectroscopy allowed the calculation of $\Delta G^{\neq}_{coal}$ values for this gross dynamic process (see Table 2), though interpretation remains speculative.

The room temperature ^{1}H NMR spectrum of the *t*Bu-substituted-Cp allyl–yttrium complex **8** in [D_8]toluene is consistent with C_1 symmetry of the molecule. The AX_4 pattern observed for the allyl protons also points to the above-mentioned dynamic processes. However, no significant change in the spectra was observed in the temperature range 233–333 K.

The ^{13}C NMR signals (25 °C, [D_8]toluene) for the bridgehead carbon atom of the fluorenyl moiety in allyl complexes appear at δ 93.8 in **2**, 91.5 in **8**, and 75.7 ppm in **12**. These values are to be compared to the chemical shifts reported for the corresponding carbon in $[(\eta^5,\eta^3\text{-Cp-CMe}_2\text{-Flu})_2\text{La}]^-[\text{Li}(\text{OEt}_2)_2]^+$ (δ 95.9 ppm),[23] $[(\eta^5,\eta^3\text{-Cp-CMe}_2\text{-Flu})\text{Zr}(\mu\text{-H})(\text{Cl})]_2$ (δ 95.9 ppm),[41] and $[(\eta^3,\kappa^1\text{-Flu-SiMe}_2\text{-N}t\text{Bu})\text{YCH}_2\text{SiMe}_3(\text{THF})]$ (δ 82.9 ppm),[42] and suggest that the reduced η^3-coordination of the fluorenyl ligand, as observed in the solid-state structures of **4**, **9**, and **12** (Figures 2–4), is retained in solution.[43]

Homopolymerization of styrene catalyzed by allyl *ansa*-lanthanidocene complexes: Allyl complexes **2–5**, **8**, **9**, **12** and **13** are active in styrene polymerization under mild conditions in the absence of any co-activator, giving highly syndiotactic polystyrene (sPS). Representative results are reported in Table 3.

The reactions proceed either in bulk styrene or in hydrocarbon solutions, which can be used to dilute the monomer. As a matter of fact, polymerizations of bulk styrene at 60 °C led to 70–85 % maximum monomer conversions. Since sPS is not soluble under the reaction conditions and precipitate during polymerization, mass transfer limitations likely take place, which may cause eventually reduction of the polymer yield. Cyclohexane was found to be an effective solvent to tackle this issue, but introduction of an aromatic hydrocarbon such as toluene in the polymerization medium proved

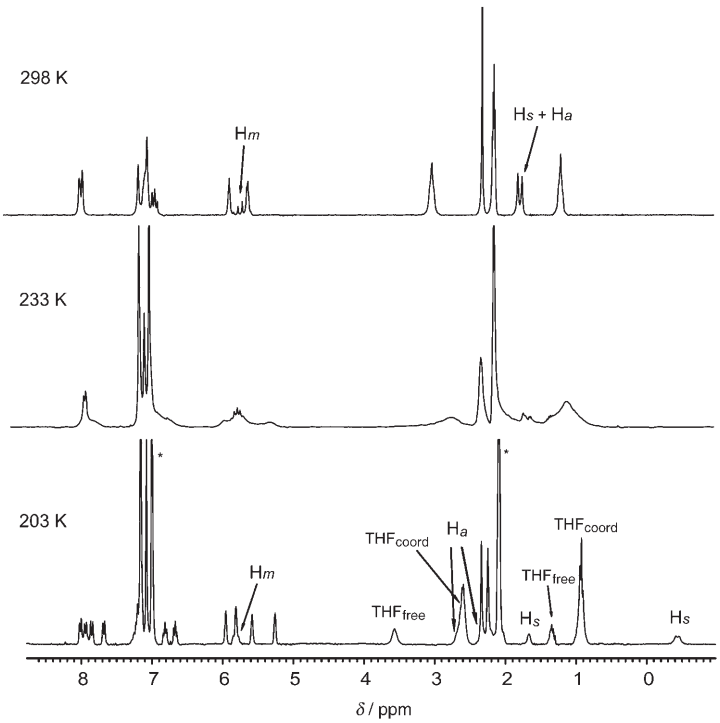

Figure 4. Variable temperature ^{1}H NMR spectra of complex **2** (300 MHz, [D_8]toluene) (* labels refer to residual solvent resonances).

Table 2. Selected ^{1}H (300 and 500 MHz) and ^{13}C (75 and 125 MHz) NMR data for allyl groups in complexes **2**, **3**, **8** and **12** ([D_8]toluene, 298 K) (chemical shifts in ppm and coupling constants in Hz).

	2	**3**[35]	**8**	**12**
$H_{methyne}$	5.63 (q, $^3J_{H,H}=12.0$) 4.66 (q, $^3J_{H,H}=11.8$)[a]	5.28 (br m)	6.19 (q, $^3J_{H,H}=12.2$)	5.63 (q, $^3J_{H,H}=12.1$)
$C_{methyne}$	144.5 (143.2)[a]	n/a	149.4	146.7
H_{anti}, H_{syn}	1.71 (d, $^3J_{H,H}=12.0$) 1.51 (d, $^3J_{H,H}=11.8$)[a]	1.20 (br s)	1.83 (d, $^3J_{H,H}=12.2$)	1.79 (d, $^3J_{H,H}=12.1$)
$C_{terminal}$	68.8 (57.8)[a]	n/a	70.4	69.5
T_{coal} [K]	≈223	n/a	–	≈218
$\Delta G^{\neq}_{coal}$[b]	11.8 ± 0.9	n/a	–	11.1 ± 0.5

[a] In [D_8]THF. [b] $\Delta G^{\neq}_{coal}$ in kcal mol^{-1} calculated from T_{coal} of the Me_2E group.

Table 3. Styrene homopolymerization catalyzed by allyl *ansa*-lanthanidocene complexes.[a]

Entry	Cpd.	[St]/[Ln]	T_{polym} [°C]	t [min]	Yield[b] [%]	Activ.[c]	M_n[d] [10^{-3}]	M_w/M_n[d]	T_m[e] [°C]
1	**2**	800	20	120	26	10	24	2.3	260
2[f]	**2**	800	60	20	8	13	15	1.6	262
3[f]	**2**	800	60	40	20	17	19	1.8	262
4[f]	**2**	800	60	60	26	14	22	1.9	262
5[f]	**2**	800	60	120	41	11	43	2.1	263
6[g]	**14**/allylMgCl	1000	60	80	62	48	12	1.2	265
7	**3**	600	20	240	14	2	48	4.7	260
8	**3**	600	60	5	16	118	20	1.2	257
9	**4**	600	20	60	33	23	66	1.4	260
10	**4**	600	60	2.5	11	448	21	1.2	262
11	**4**	600	60	3.5	34	989	35	1.3	nd
12	**4**	600	60	4	45	1145	50	1.3	261
13	**4**	600	60	5	84	1710	54	1.7	264
14	**4**	500	120	2[h]	100[h]	>1733[h]	26	2.2	nd
15	**4**	2300	60	5	9	256	62	1.5	nd
16	**4**	2300	60	10	64	911	116	1.9	nd
17	**4**	2300	60	30	72	342	135	2.1	263
18	**4**	4000	60	30	28	222	128	2.6	nd
19	**5**	600	60	5	28	218	27	1.5	262
20	**8**	2000	60	1440	11	1	28	2.7	261
21	**9**	600	60	240	6	1	4	8.9[i]	nd
22	**12**	500	60	2880	13	<1	37	15.2[i]	nd
23	**13**	500	60	35	35	32	24	1.9	255
24	**13**	800	100	5	21	195	9	1.9	251
25[j]	$CpTiCl_3$/MAO	4500	60	2	76	102000	76	2.1	263

[a] General conditions unless otherwise stated: 3–7.10^{-5} mol of Ln complex; 8.70 mol L^{-1} (bulk) styrene; The results shown are representative of at least duplicated experiments. [b] Isolated yield of sPS collected after precipitation in MeOH. [c] Catalytic activity in kg sPS mol Ln^{-1} h^{-1} calculated over the whole reaction time. [d] Number average molecular weight and polydispersity determined by GPC in 1,3,6-trichlorobenzene at 135 °C versus PS standards. [e] Melting temperature of PS measured by DSC. [f] Reactions carried out in toluene (5 mL). [g] [(Cp-CMe_2-Flu)Y(μ-Br)]$_2$ (**14**) was treated in situ with dried (allyl)MgCl (1 equiv vs Y). [h] Reaction time was not optimized. [i] Bimodal distributions. [j] [Al]/[Ti] = 1000.

to be detrimental, leading to significantly lower catalyst activity. Likely, this decrease in polymerization activity could stem from competitive coordination of toluene onto the metal center that blocks the subsequent attack of the π-system of the styrene vinyl group of incoming monomer units.[44] Polymerizations of bulk styrene offer the most convenient procedure with overall performances in terms of control similar to those in cyclohexane solutions. Though the polymerizations proceed from 20 °C (Table 3, entries 1 and 7), valuable activities were observed only above 60 °C (see below). The polymerization activity of allyl *ansa*-lanthanidocenes **2–5** is in the order Nd ≫ Sm > La > Y (entries 1–19). The maximum turnover frequency (TOF) value for yttrium complex **2** at 60 °C, in bulk, was estimated to be 380 h^{-1} (calculated over 60 min), whereas the TOF value observed for the parent neodymium complex **4** is 8830 h^{-1} under similar conditions (entry 16; calculated over 10 min). Although an optimal apparent polymerization activity for the neodymium complex is not unexpected in light of literature,[17] this activity trend does not follow the order of the metal ionic radii.[45] We assume it may also reflect, at least in part, the instability of some of the complexes under the polymerization conditions, particularly in the case of lanthanum complex **3**.[46] It is noteworthy that styrene polymerizations mediated by complexes **2–5** all feature an induction period (Figure 5). When the polymerization temperature was raised from 50 to 60 °C, using complex **4** as catalyst, a significant increase in activity was observed, which is greater than that expected from the simple influence of temperature on kinetics. These observations suggest the existence of a pre-activation step, possibly related to dissociation of a THF molecule from the metal center in the pre-catalyst. Full monomer conversion can be achieved within two minutes ([St]/[Ln] = 500) upon carrying out bulk polymerization at 120 °C with neodymium complex **4** (entry 14). This catalyst system appears remarkably robust at such a high temperature, since no formation of atactic polystyrene (which would evidence a radical polymerization contribution) was observed (see below).

The average number molecular weights (M_n) of the sPS obtained with these systems are in the range 6000 to 135000 g mol^{-1}. The molecular mass distributions are rather narrow, ranging usually from 1.2 to 2.1, which indicates a single-site catalyst behavior. Larger polydispersities ($2.1 < M_w/M_n < 5.2$) have been determined only for sPS samples produced over relatively long periods (usually > 60 min; see for instance entry 7) or at high monomer-to-catalyst ratios (see for instance entry 18), which may arise from either the aforementioned mass-transfer limitations and/or

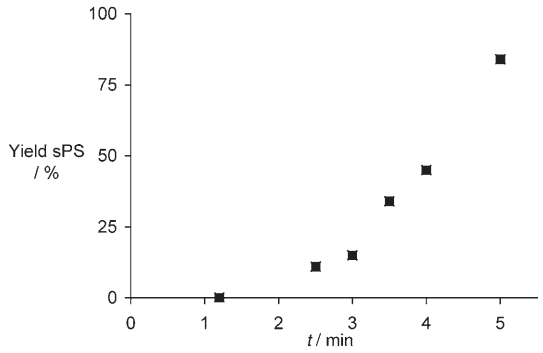

Figure 5. Dependence of sPS yield versus time for the styrene polymerization promoted by complex **4** (60 °C, [St]/[Nd] = 600, bulk).

from gradual catalyst decomposition with time. The experimental M_n values are systematically lower than those calculated (for $M_w/M_n < 1.3$), reflecting a moderate initiation efficiency (ca. 33–56%). The dependence of the molecular weights M_n versus monomer conversion for polymerization reactions catalyzed by the yttrium and neodymium complexes **2** and **4**, respectively, in toluene solution and in bulk styrene, is shown in Figure 6. These plots appear approximately linear in the first stage, indicative of a controlled polymerization, but show afterwards a saturation limit, possibly reflecting transfer reactions.

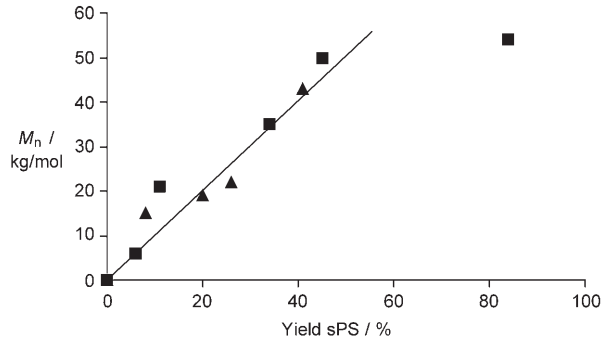

Figure 6. Dependence of M_n vs. PS yield; ▲: complex **2**, 60°C, [St]/[Y] = 800, toluene solution (Table 3, entries 2–5); ■: complex **4**, 60°C, [St]/[Nd] = 600, bulk (Table 3, entries 10–13).

Poor productivity for styrene homopolymerization was achieved using allyl complexes **8**, **9**, **12** and **13** (Table 3, entries 21–30). Neither rising the polymerization temperature nor conducting the reaction for longer time periods did improve significantly the polymer yields. It is reasonable to assume that steric and possibly electronic features in these species may be detrimental to polymerization activity. As a matter of fact, the poorest activity is observed with complexes **8** and **9**, which are derived from the most sterically demanding ligand. Also, the silylene-bridged complexes **12** and **13** feature much larger bite angles than their isopropylidene-bridged parents (see above), an obvious steric parameter that is also known to affect global electronics of the molecule and in turn possibly their reactivity.[27]

The polystyrenes obtained with all these allyl *ansa*-lanthanidocenes, especially complex **4**, feature a highly syndiotactic microstructure. A typical $^{13}C\{^1H\}$ NMR spectrum of a non-fractionated (crude) polymer sample obtained for complex **4** at 60°C is shown in Figure 7. A single sharp resonance at δ 145.6 ppm is observed, which is assigned to the phenyl *ipso*-carbon of sPS, giving a *rrrr* pentad abundance of $\geq$ 99%.[4b] Remarkably, crude polystyrenes produced with this catalyst system at temperatures as high as 120°C (Table 3, entry 14) feature the same type of spectrum, indicating that the samples are not contaminated by atactic polystyrene (which could be produced by thermally self-initiated polymerization[47]). The high syndiotacticity of the polystyrenes is also illustrated by the high T_m of 250–268°C, which are usual values for sPS.[48] Also, the glass transition temperature (T_g = 111.5°C) and the Young modulus (E = 2320 MPa at 35°C), both determined by dynamic mechanical analysis (DMA), compare well with the corresponding values determined under the same conditions (T_g = 110.8°C; E = 2920 MPa at 30°C) for a sPS sample prepared independently with the $CpTiCl_3$/MAO system (Table 3, entry 25).

Styrene–ethylene copolymerization catalyzed by allyl *ansa*-lanthanidocenes: The allyl complexes prepared have also been used for the copolymerization of styrene with ethylene, with the aim to prepare microstructurally controlled styrene-rich copolymers. Initial investigations were intended at evaluating the performance of complexes **2**, **4** and **9** in ethylene homopolymerization. Despite their high efficiency in polystyrene production, **2** and **4** were found to be quite poor catalysts for ethylene polymerization. No activity was observed using yttrium–allyl **2** (toluene, 80°C, 5 atm), whereas its neodymium counterpart **4** polymerizes sluggishly ethylene (24 kg mol^{-1} h^{-1} in toluene, 60°C, 5 atm) to yield low molecular weight products (M_n = 1000, M_w/M_n = 2.0, T_m = 128°C). In contrast, being poorly active towards styrene, complex **9** shows significant activity in ethylene polymerization, though, under relatively severe conditions (900 kg mol^{-1} h^{-1} in cyclohexane, 80°C, 8 atm).

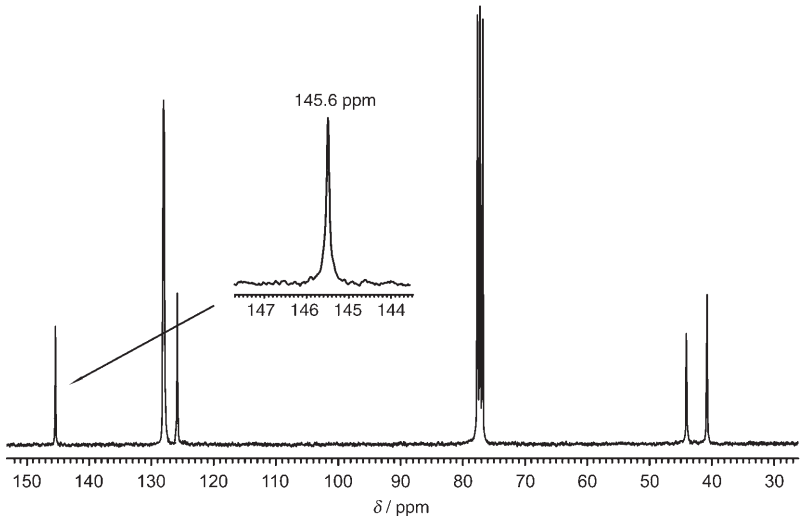

Figure 7. $^{13}C\{^1H\}$ NMR spectrum (125 MHz, 60°C, $CDCl_3$) of sPS obtained with complex **4** (Table 3, entry 9).

Next, a series of screening experiments was conducted to evaluate the performance of the prepared allyl complexes in

Table 4. Styrene–ethylene copolymerization catalyzed by allyl *ansa*-lanthanidocene complexes **4**, **9** and **13**.[a]

Entry	Cpd.	[St]/[Ln]	[St] [M] (*m*, [g])[b]	*p* [bar]	*T* [°C]	*t* [min]	Yield[c] [g]	Activ.[d]	St.[e] [mol %]	M_n[f] [10^3]	M_w/M_n[f]	T_m[g] [°C]	T_g[h] [°C]
26	**4**	600	8.7 (9.06)	1	60	10	6.8	277	97±2	25	3.2	231	85
27	**4**	600	8.7 (9.06)	1	80	5	8.4	674	97±2	23	3.8	223	66
28	**4**	600	8.7 (9.06)	1	100	3	8.4	1082	91	15	2.5	218	71
29	**4**	600	4.3 (9.06)	1	60	17	5.6	129	97±2	72	1.6	232	100
30	**4**	600	4.3 (9.06)	1	80	18	8.4	191	97±2	78	1.7	241	63
31	**4**	600	4.3 (27.2)	4	60	30	9.8	44	71	73	1.2	nd	77
32	**4**	600	2.2 (9.06)	1	60	120	7.4	26	90	114	1.8	–	100
33	**4**	600	2.2 (13.59)	4	60	120	4.9	11	54	93	1.4	–	65
34	**4**	600	2.2 (9.06)	8	60	120	4.1	15	45	21	3.1	nd	45
35	**4**	600	1.2 (1.81)	1	60	120	0	0	–	–	–	–	–
36	**4**	1000	8.7 (2.27)	1	120	1.5	1.5	2529	97±2	9	2.4	214	71
37	**4**	1100	8.7 (54.3)	5	80	40	25.8	85	90	144	1.5	–	nd
38	**4**	1100	4.3 (54.3)	5	60	30	43.8	228	76	143	1.6	–	79
39	**4**	1100	2.4 (18.1)	5	60	20	11.4	240	60	98	1.5	–	65
40	**4**	1300	2.4 (18.1)	2	60	120	14.2	53	78	124	1.7	205	91
41	**4**	3000	8.7 (45.3)	1.5	60	20	9.4	218	97±2	75	2.2	233	91
42	**4**	3000	8.7 (45.3)	4	60	30	14.5	225	84	137	1.8	–	70
43	**4**	3000	8.7 (54.3)	5	80	20	19.6	338	94	152	1.4	–	89
44	**4**	7400	8.7 (54.3)	5	100	80	0.4	6	97±2	46	1.5	–	–
45	**9**	500	8.7 (3.62)	1	80	60	0.02	<1	92	nd	nd	nd	nd
46	**13**	550	8.7 (0.91)	1	100	60	0.04	3	97±2	nd	nd	nd	nd

[a] General conditions: 0.02–0.15 mmol Ln, total volume 2–60 mL; reactions were conducted either in bulk styrene ([St] = 8.7 M) or in cyclohexane solution (1.2 < [St] < 4.3 M); The results shown are representative of at least duplicated experiments. [b] Styrene concentration (in mol L^{-1}) and mass of styrene initially introduced (in g). [c] Mass of copolymer recovered. [d] Catalytic activity in kg mol $Ln^{-1} h^{-1}$. [e] Amount of styrene incorporated in the copolymer, as determined by ^1H NMR; "±2" refers to the experimental uncertainty in determining the ethylene content in styrene-rich copolymers. [f] Number average molecular weight and polydispersity determined by GPC in 1,3,6-trichlorobenzene at 135 °C versus PS standards. [g] Melting temperature as determined by DSC (2nd pass); "–" indicates that no melting transition was detected. [h] Glass transition temperature as determined by DMA (at 30 °C).

styrene–ethylene copolymerization. These tests revealed the remarkable activity of neodymium complex **4**, which efficiently copolymerizes styrene and ethylene to statistic poly(styrene-*co*-ethylene) with unprecedented high styrene contents (>95–97 mol %). Table 4 summarizes representative results obtained upon varying the reaction temperature, styrene concentration and styrene/ethylene feed ratios. Since the use of toluene as solvent for styrene homopolymerization was previously found to be detrimental in terms of activity (see above), copolymerization reactions were carried out either in bulk styrene or in cyclohexane solutions.

The copolymers isolated after a standard work-up are true copolymers, that is, not mixtures of homopolymers of styrene and ethylene, and therefore do not require further fractionation.[49] This is first evidenced by the fact that the copolymers feature monomodal molecular weight distributions in size-exclusion chromatography (SEC) analysis, using dual UV/refractive index (RI) detections. More, the copolymer distributions obtained from Temperature Rising Elusion Fractionation (TREF) analysis are indicative of their homogeneous composition (Figure 8). The polydispersities are generally narrow ($M_w/M_n \approx 2$), suggesting a single-site polymerization mode.

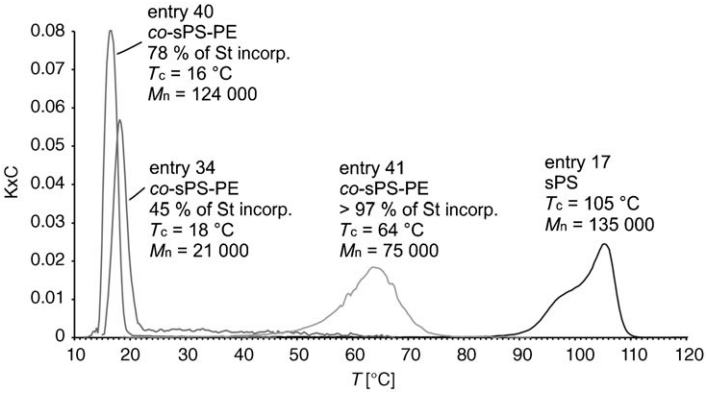

Figure 8. Crystallizability distributions as determined by Temperature Rising Elusion Fractionation (TREF) analysis (see Experimental Section for details).

The following findings, derived from analysis of data obtained with complex **4** and in part reported in Table 4, evidence the flexibility and limits of the copolymerization process:

a) The apparent catalytic activity (calculated over the whole polymerization time) increases with the styrene concentration (Figure 9) (compare also Table 4, entries 26/29/32 and 27/30). Though, no polymerization takes place at a low styrene concentration of 1.2 M at 60 °C (entry 35), most likely because the allyl *ansa*-lanthanidocene is not soluble under these conditions;

b) the average-number molecular weights of the copolymers increase monotonously, though slightly, with the [styrene]/[Ln] ratio, while the polydispersities remain relatively narrow (compare for instance entries 31/38, 32/40, 26/41). Complex **4** proved to be productive even up to [styrene]/[Nd] ratio of 7,400 (entry 44) but at the expense of catalytic activity;

c) the amount of styrene incorporated in the copolymers is readily adjustable over a wide range, depending on the conditions used, that are mainly the styrene concentration and ethylene pressure. At high [styrene]/[ethylene] ratio, that is, bulk styrene and moderate ethylene pressure, incorporation of styrene up to 97 ± 2 mol% can be achieved (Figure 10) (entries 26, 27, 29, 30, 36, 41), which represents to our knowledge the highest value documented so far in P(S-*co*-E) copolymers. On the other hand, the ethylene content in the copolymers increases, as expected, upon rising the pressure (Figure 11) (compare also entries 29/31, 32/33/34, 36/37/39/40), reaching readily up to 45 mol%;

d) temperature has a pronounced influence on the catalytic performance and properties of the copolymers. The activity rises up by one order of magnitude when going from 60 to 120°C (entries 26/36, maximal activity of 2530 kg P(S-*co*-E) $mol^{-1} h^{-1}$ at 120°C); notably, the thermal stability of the *ansa*-lanthanidocene catalyst up to 120°C, which is quite unusual. As expected, the molecular weights of copolymers decrease gradually with increasing temperature (compare for instance entries 26/27/28/36), but high molecular weight polymers can be readily recovered at 80°C (entries 37, 43).

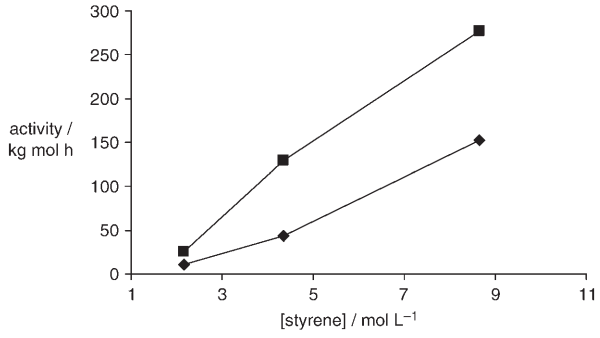

Figure 9. Influence of styrene concentration on polymerization activity in the ethylene–styrene copolymerization promoted by **4**: ■: 1 bar, ◆: 5 bar (80°C, bulk or cyclohexane solution; see Table 4 for other conditions).

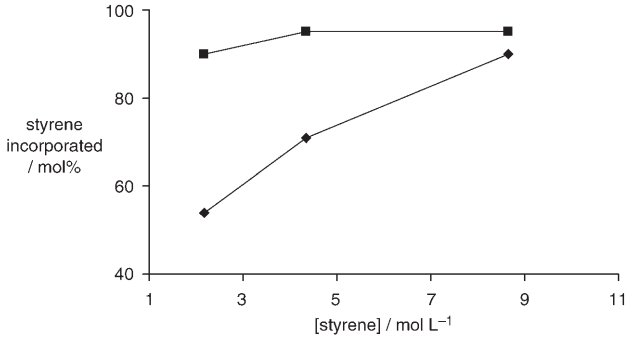

Figure 10. Influence of styrene concentration on the styrene incorporation in ethylene–styrene copolymerization promoted by **4**: ■: 1 bar, ◆: 5 bar (bulk or cyclohexane solution; see Table 4 for other conditions).

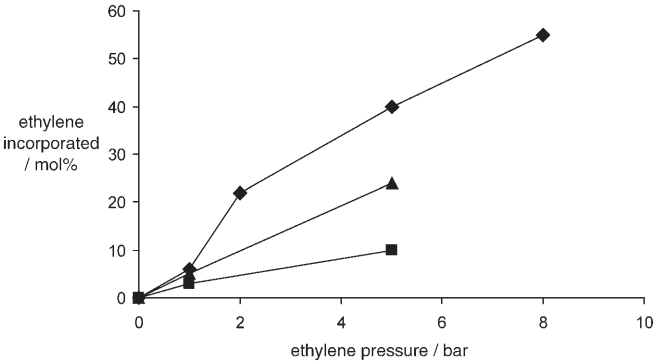

Figure 11. Influence of ethylene pressure on ethylene incorporation in the ethylene–styrene copolymerization promoted by **4** (see Table 4 for conditions); ◆: cyclohexane, 60°C, St/Ln = 600, [St] = 4.35 M; ▲: cyclohexane, 80°C, St/Ln = 600, [St] = 4.35 M; ■: neat styrene, 60°C, St/Ln = 600, [St] = 8.7 M.

In striking contrast with complex **4**, allyl *ansa*-neodymocenes **9** and **13** that bear *t*Bu-substituted and silylene-bridged ligands, respectively, revealed to be poorly active for styrene–ethylene copolymerization (Table 4, entries 45, 46). As for styrene homopolymerization, we assume that this decrease in activity stems from the higher steric crowding induced by these ligands and, consequently, the more hindered coordination sphere of the metal center that makes the approach of the monomer(s) more difficult. Also, electronic considerations cannot be discarded in the case of **13**.

Microstructure of styrene–ethylene copolymers: ^{13}C NMR spectroscopy allowed us to clarify the microstructure of the prepared styrene–ethylene copolymers using previously reported assignments.[8,12] Possible monomer sequences available in styrene-enriched poly(styrene-*co*-ethylene) copolymers are depicted below (S* refers to possible head-to-head and tail-to-tail misinsertions of styrene units), while the ali-

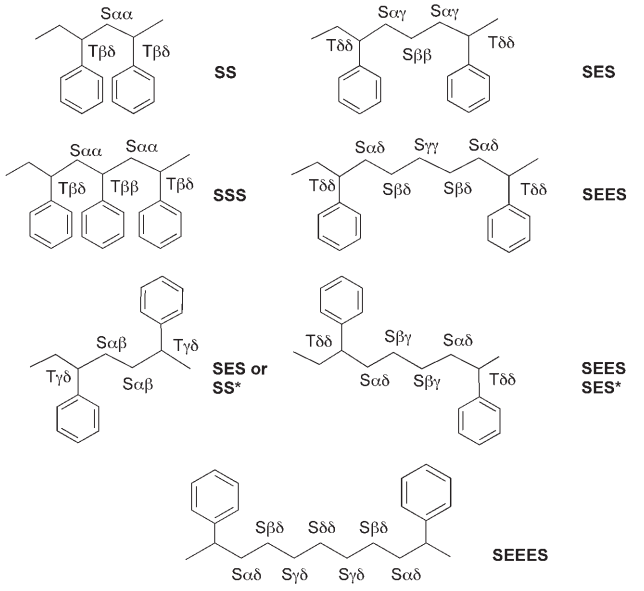

phatic regions of the $^{13}C\{^1H\}$ NMR spectra of four samples with variable content of incorporated ethylene are shown in Figure 12. The overall pattern of signals remains persistent despite of the gradually changing content of ethylene incorporated in those four copolymers, and is consistent with the presence of single ethylene units or very short ethylene sequences randomly distributed over the polymer chain. For instance, for an ethylene-rich copolymer (Figure 12a, 55 mol% ethylene content), several resonances assigned to SEES (δ 27.1 ppm), ESSE (δ 37.9, 38.1, 43.1 ppm), and ESE (δ 37.1 ppm) sequences are observed, along with a low intensity resonance attributable to a EEE/EESEE sequence (δ 29.9–30.1 ppm). The latter is no longer observed in the spectra of the copolymer samples that feature higher styrene contents (Figure 12b–d).[50] For those styrene-rich copolymers, the $^{13}C\{^1H\}$ NMR spectra show an increase in the intensity of the resonances attributable to SSSE and SSSS sequences (δ 40.7–42.9 ppm). The most interesting observation is that the polystyrene sequences are highly syndiotactic, regardless the content of incorporated ethylene. In order to evaluate the degree of syndiotacticity of the polystyrene units in the copolymer with high ethylene content (45 mol%; Table 4, entry 34), a "quantitative" $^{13}C\{^1H\}$ NMR spectrum was recorded using an appropriate parameters set (see Experimental Section). The aromatic *ipso*-carbon region of the corresponding spectrum contained a strong resonance accounting for >81% which is assigned to syndiotactic polystyrene diads *r* (δ 145.5–145.6 ppm), along with minor resonances (δ 146.1–146.2 ppm, to be correlated with other resonances at δ 45.3–45.7 ppm).[51] Those minor resonances are no longer observed in the spectra of copolymers with higher styrene contents (Figure 12c–d), which may suggest that higher stereocontrol of styrene insertion takes place at higher styrene feed.[51]

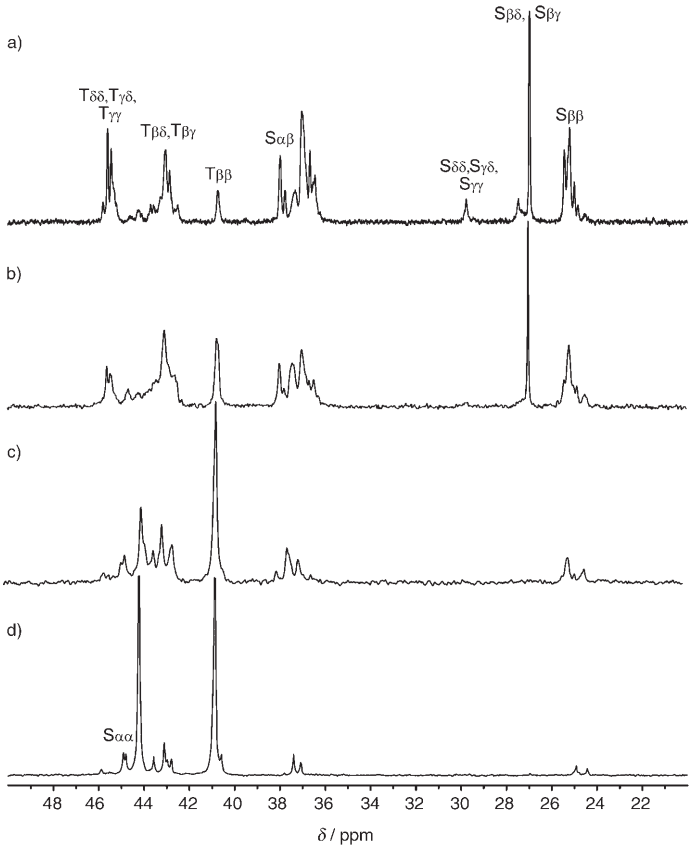

Figure 12. Aliphatic region of $^{13}C\{^1H\}$ NMR spectra (75 MHz, 25°C, $CDCl_3$) recorded for poly(styrene-*co*-ethylene) copolymers: a) 45 mol% of styrene; Table 4, entry 34; b) 60 mol% of styrene, entry 39; c) 84 mol% of styrene, entry 42; d) 97±2 mol% of styrene, entry 29.

Preliminary differential scanning calorimetry (DSC), dynamic mechanical (DMA) and TREF analyses have shown that the thermophysical properties of the poly(ethylene-*co*-styrene) copolymers prepared in this study strictly depend on their composition. Typically, ethylene-rich copolymers (i.e., ethylene >20 mol%) feature no distinct melting point in DSC thermograms. The melting temperatures determined for styrene-rich copolymers (i.e., ethylene <20 mol%) range from 205 to 233°C, and significantly differ from that of syndiotactic homopolystyrenes (257–268°C) obtained with the same catalyst.[48] It is reasonable to assume that this difference stems from the aforementioned absence of long sPS blocks in these P(S-*co*-E) copolymers. The data reported in Table 4 suggest qualitatively that the lower the ethylene content, the higher the melting temperature of the copolymer; though, comprehensive studies are still required to further establish this trend. As it is clearly seen from the TREF data (Figure 8), the crystallization temperature of copolymers also increases with increasing content of syndiospecifically enchained styrene units. The glass-transition temperatures were determined by DMA and found, as expected, to be also dependent on the ethylene/styrene ratio. For two series of copolymers prepared, respectively, in cyclohexane solution and in bulk styrene, the T_g values were found to increase significantly with the styrene content (Figure 13) (see also Table 4). Noteworthy, the T_g values of these new copolymers (T_g=45–100°C) appear quite higher than those reported for ESI materials (T_g=−23 to +58°C).[52]

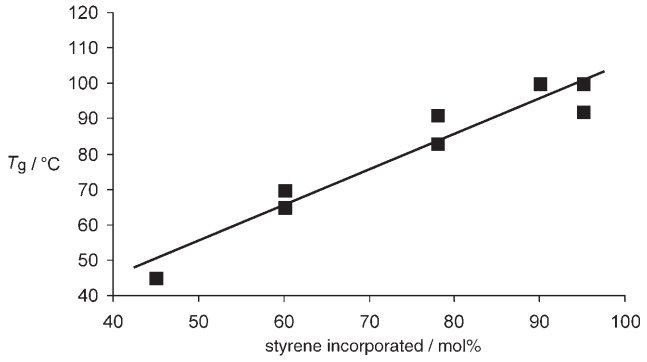

Figure 13. Evolution of glass transition temperature (T_g) in poly(styrene-*co*-ethylene)s prepared in cyclohexane with complex **4** (Table 4, entries 29, 32, 34, 39 and 40).

Discussion

Nature of the active species and initiation step: The nature of the "true" active species in syndiospecific polymerizations of styrene is still being debated. In the titanium-mediated processes, those are believed to be Ti^{III} species, generated upon in situ reduction of the parent Ti^{IV} pre-catalysts.[53,54] Recently, Hou et al. reported perfectly syndiospecific styrene polymerization using the binary system $[(Me_3SiC_5Me_4)Ln(CH_2SiMe_3)_2(THF)]/[Ph_3C][B(C_6F_5)_4]$ (Ln = Sc, Y, Gd, Lu).[8] In both the Ti and Ln case, isolobal species of general composition $Cp'M(R)^+$ (Cp′ = (non)substituted cyclopentadienyl or indenyl; M = Group 3, 4 metal; R = alkyl group) could be assigned to represent the active form of the catalyst. Those species have no relevance to the active species issued from neutral *ansa*-lanthanidocenes [{Cp-CMe_2-Flu}LnR(THF)], since this would imply cleavage of either the Ln–Cp or Ln–Flu bonds, which is unlikely. Rather, we suggest that the actual catalytically active species for syndiospecific styrene (co)polymerization mediated by allyl *ansa*-lanthanidocenes **A** may be unsaturated and/or weakly coordinated neutral species **B** or **C** depicted in Scheme 2. Dissociation of the THF molecule from pre-catalyst **A** to produce base-free complex **B** is likely of crucial importance, and refers to some above mentioned experimental observations, that is, the fluxional behavior of allyl complexes **2** and **12** in solution as evidenced by VT NMR, and the existence of an induction period in styrene homopolymerization (Figure 5).

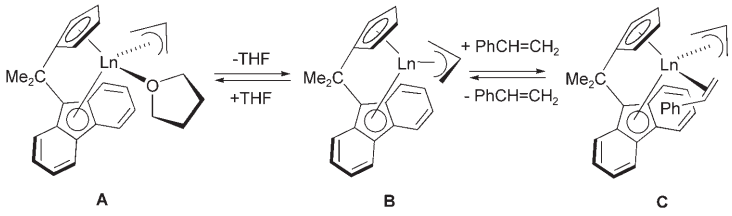

Scheme 2. Possible generation of catalytically active species for syndiospecific styrene (co)polymerization.

On the other hand, we assume that the role of the allyl group is essential for the initiation step. Our previous investigations, when exploring the catalytic performance of parent yttrium complexes derived from the $[Cp\text{-}CMe_2\text{-}Flu]^{2-}$ ligand, revealed that complexes such as the dimeric hydride $[\{(Cp\text{-}CMe_2\text{-}Flu)\}Y(\mu\text{-}H)(THF)]_2$, and sterically crowded monomeric alkyl complexes [{Cp-CMe_2-Flu}$Y(CH(SiMe_3)_2)$(THF)] and [{Cp-CMe_2-Flu}$Y(CH_2SiMe_3)$(THF)], are inert towards both styrene and ethylene.[15] On the other hand, $[(Cp\text{-}CMe_2\text{-}Flu)Y(\mu\text{-}Br)]_2$ (**14**),[24] when treated with (allyl)MgCl (1 equiv vs Y, as a THF solution) to generate the corresponding allyl yttrium complex in situ, affords sPS with good activity and a relatively narrow molecular weight distribution (Table 3, entry 6).[55]

A chain-end analysis was undertaken to establish whether the allyl ligand is the initiating group in the polymerization process. In fact, the ^1H NMR spectrum of a relatively low molecular weight sPS polymer ($M_n = 6000\ g\,mol^{-1}$ as determined by GPC) prepared from complex **4** featured two signals at δ 5.59 (1H) and 4.81 ppm (2H) that are characteristic for the vinyl moiety of an allyl end group.[56] Also, the high resolution MALDI-TOF-MS data of this sPS sample (Figure 14) are in agreement with both the theoretical molecular weight for allyl-terminated chains and experimental results from GPC; a single Gaussian distribution is observed and the molecular weight of each peak is consistent with the calculated molecular weights for the on-matrix compounds $(H)(C_8H_8)_n(C_3H_5)Ag$, where *n* represents the degree of polymerization.

It is well known that the regioselectivity of syndiotactic styrene polymerization mediated by organotitanium compounds is extremely high. Both the very first initiative insertion step in the metal–alkyl bond and all the subsequent styrene enchainments proceed via secondary insertion.[57] The subsequent elementary steps (that constitute propagation) strongly interrelate with and constitute the ground for the syndiospecific incorporation of styrene; that is, the repulsion generated by the phenyl ring of the last 2,1-inserted styrene molecule guides the secondary coordination and further stereoselective incorporation of the next incoming monomer unit.

However, the degree of stereocontrol provided by the allyl *ansa*-lanthanidocenes investigated in the present study in syndiospecific polymerization of styrene is unprecedently high. In fact, complex **4** still promotes the formation of highly syndiotactic polystyrenes under conditions that proved to be unacceptable for traditional sPS production (e.g., polymerization temperatures of 100–120 °C).[4a] In order to find out the origin of the stereocontrol afforded by these allyl *ansa*-lanthanidocenes, a statistical analysis of a relatively less stereoregular sPS sample obtained at 120 °C was conducted. As depicted in Figure 15, the aromatic *ipso*-carbon region of the high-field ^{13}C NMR spectrum shows only four distinct signals assigned to one major *rrrrrr* and three minor *rrmrrr*, *rmrrrr* and *mrrrrr* heptads.[58] The relative intensities of those, 0.74, 0.09, 0.09 and 0.09, respectively, perfectly match with the first-order Markovian (Bernoullian) statistics of the chain-end stereocontrol.[59] The examination of the methylene carbon region at the pentad level corroborated the statistical analysis.[60] Another point that supports chain-end control as the main stereocontrol mechanism is the fact that highly syndiotactic polystyrene (*rr* > 99%, as determined by ^{13}C NMR spectroscopy)[61] is produced using allyl–neodymium complexes bearing a C_1 symmetry ligand geometry,[62] for example, complexes **8** and **9** (Table 3, entries 20, 21).

In addition to this main chain-end control mechanism, we assume that the geometry of the active site influences also the stereoselectivity of styrene enchainment; that is, enantiomorphic site control contributes to the very high syndiotacticities observed, even at high temperatures. The detailed

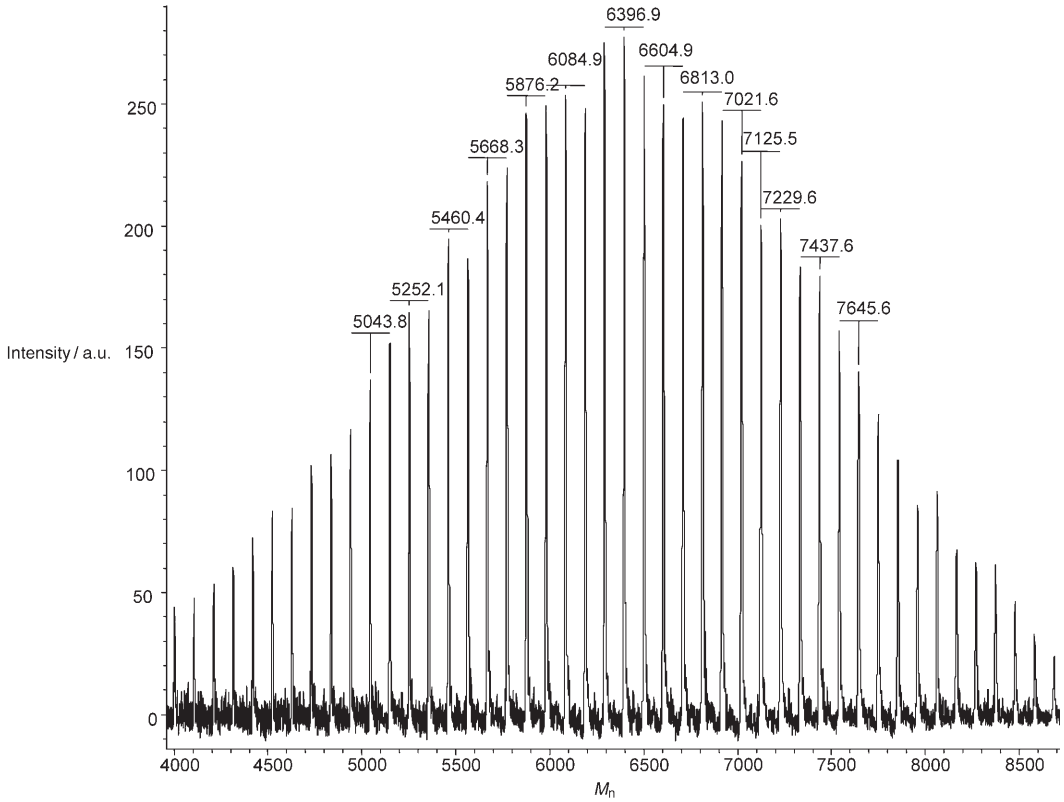

Figure 14. High resolution MALDI-TOF mass spectrum of a sPS ($M_n = 6000\ g\,mol^{-1}$ as determined by GPC) produced from complex **4** (polymer doped with AgOTf, dithranol matrix).

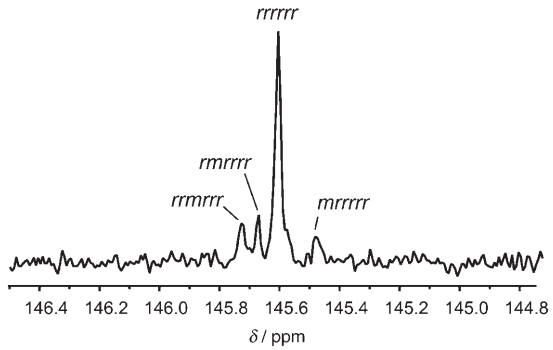

Figure 15. Region of the *ipso*-phenyl carbon of the $^{13}C\{^1H\}$ NMR spectrum (500 MHz, 60 °C, $CDCl_3$) of a sPS sample obtained at 120 °C with complex **4** (Table 3, entry 14).

mechanism of stereospecific styrene polymerization mediated by various Ti^{III} species has been investigated by Cavallo[63] and Jo[64] using theoretical studies at the DFT level. Those computations were intended at rationalizing the intrinsic role of the chiral orientation of the growing polymeric chain on the regio- and stereoselectivities of the insertion step, using as model geometries such ligand–metal frameworks such as [CpTi], [(benzene)Ti] and [*ansa*-Me_2SiCp_2Ti]. However, in line with the initial objectives of those theoretical studies, no possible impact of the geometry of the active site was assessed. In our case, we may reasonably propose two possible geometries for styrene enchainment via 2,1-insertion (Scheme 3).[65] The growing polymer chain, stabilized by π-agostic interactions between phenyl rings and the active center[63,64] on one enantioface of the pseudo-C_s-symmetric molecule, orientates in a way to minimize interactions with the fluorenyl part of the ligand. This orientation induces chirality at the metal center (only one enantiomer form of the complex is depicted in Scheme 3) and, in turn, a preferable coordination of styrene (*Re* and *Si* enantiofaces), that is the one that features minimal steric repulsion of the phenyl ring with the fluorenyl group of the ligand (i.e., *Re* in Scheme 3a). In this situation, the upcoming migratory insertion will create a new chiral carbon atom with an absolute configuration opposite to the penultimate unit of the growing polymer chain, and the vacant coordinating position will appear on the opposite enantioface of the active species to accommodate a styrene molecule on the opposite enantioface (i.e., *Si* in Scheme 3a).

This possible additional contribution of an enantiomorphic-site control mechanism may also account for the observed high stereocontrol in styrene–ethylene copolymerization.[66] As for styrene homopolymerization, each time a styrene unit enchains via secondary insertion, the following styrene incorporation will produce highly syndiotactic sequences. However, when an ethylene unit is enchained, ethylene and styrene will compete for the subsequent insertion step. Considering the higher propensity of these *ansa*-lanthanidocenes

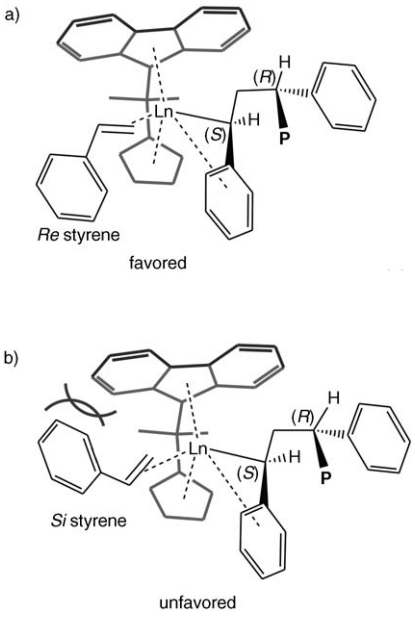

Scheme 3. Possible contribution of enantiomorphic-site control (only one enantiomer form of the complex is depicted)

to polymerize styrene rather than ethylene, the active species will likely accommodate at this stage a styrene molecule; this is consistent with the experimentally observed low amount of multiple ethylene sequences in the copolymers (see above). However, chain-end control is inoperative at this point and the high syndiotacticity that is maintained in the polystyrene sequences (as observed by ^{13}C NMR) may originate from contribution of the enantiomorphic site control.

More precise and reasonable mechanistic details could be given only after comprehensive theoretical investigation of this prominent intriguing catalytic system.

Comparison of single-component versus binary Group 3 metal catalyst systems: It is worth comparing the catalytic performance of these neutral allyl *ansa*-lanthanidocenes, as well as the microstructure of the resultant (co)polymers, with those obtained from the binary cationic system developed by Hou and co-workers (**D,** see Introduction).[8] Those two systems are obviously among the most effective catalysts to date for copolymerizing styrene with ethylene, considering activities, productivities, stereoselectivities *and* the possibility to prepare copolymers with a very high styrene content. Hou's system is very active and can be compared in this respect to the "classic" $CpTiCl_3$/MAO system. This high activity may be expected, taking into account the similar nature of active cationic species in those two systems. Neutral allyl *ansa*-lanthanidocenes are less active. Nevertheless, upon using neodymium complex **4**, styrene–ethylene copolymerization can be efficiently conducted at 100–120 °C with rates as high as those observed with Hou's cationic system at room temperature, avoiding catalyst decay and still providing excellent stereocontrol. Unprecedentedly high styrene incorporation in the poly(styrene-*co*-ethylene) structure was achieved using these discrete allyl *ansa*-lanthanidocenes. On the other hand, the microstructures of the copolymers produced with these two catalyst systems, especially for ethylene-rich copolymers, are quite dissimilar: random multiblock poly(sPS-*co*-E) structures with allyl *ansa*-lanthanidocenes versus alternating sPS-PE copolymers with the binary cationic systems.

Conclusions

A new class of neutral allyl *ansa*-lanthanidocenes [{Flu-EMe_2-(3-R-Cp)}Ln(2-R′-C_3H_4)(THF)] (E = C, Si; R = H, *t*Bu; R′ = H, Me) bearing fluorenyl/cyclopentadienyl ligands is disclosed in this contribution. These compounds (and especially **4**) appear to be effective single-component precursors to produce highly syndiotactic polystyrene with good control of the polymerization. Moreover, successful copolymerization of styrene with ethylene using **4** has been evidenced to yield poly(styrene-*co*-ethylene) copolymers composed of long highly syndiotactic polystyrene sequences connected by single or very short (poly)ethylene units. One profitable advantage of this system is that the production of styrene–ethylene copolymers is not contaminated with homopolymers. Unlike most of the other catalysts reported so far for ethylene–styrene copolymerization, those allyl *ansa*-lanthanidocenes appear to be more competent for polymerizing styrene rather than ethylene. This unique feature allows obtaining copolymers with the highest styrene content reported so far in the literature. The catalysts are highly thermally robust, enabling homo- and copolymerization processes to proceed in a broad temperature range up to 120 °C with high activities and in a controlled manner completely void of free radical-mediated counterparts.

Experimental part

General considerations: All manipulations were performed under a purified argon atmosphere using standard Schlenk techniques or in a glovebox. Solvents were distilled from Na/benzophenone (THF, Et_2O) and Na/K alloy (toluene, pentane) under nitrogen, degassed thoroughly and stored under nitrogen prior to use. Deuterated solvents ([D_6]benzene, [D_8]toluene, [D_8]THF; >99.5% D, Eurisotop) were vacuum-transferred from Na/K alloy into storage tubes. [$YCl_3(THF)_{3.5}$], [$LaCl_3(THF)_{1.5}$], [$NdCl_3(THF)_2$] and [$SmCl_3(THF)_2$] were obtained after repeated extraction of YCl_3, $LaCl_3$, $NdCl_3$ and $SmCl_3$ (Strem) from THF or just prior to use by refluxing the corresponding anhydrous lanthanide chloride in THF for 2 h and subsequent evaporation. The pro-ligands CpH-CMe_2-FluH and (3-*t*Bu-CpH)-CMe_2-FluH were generously provided by Total Petrochemicals. Complexes [(Cp-CMe_2-Flu)YCl_2]$^-$[Li(ether)$_4$]$^+$ (ether = Et_2O, THF) (**1**)[23] and [(Cp-CMe_2-Flu)Y(μ-Br)]$_2$ (**14**)[24] were prepared as reported before. The pro-ligand CpH-$SiMe_2$-FluH and complex [(Cp-$SiMe_2$-Flu)Y(μ-Cl)]$_2$ (**10**) were prepared using the reported procedures.[28] NMR spectra of complexes were recorded on Bruker AC-200, AC-300 and AM-500 spectrometers in Teflon-valved NMR tubes at 23 °C unless otherwise indicated. ^1H and ^{13}C chemical shifts are reported in ppm vs $SiMe_4$ and were determined by reference to the residual solvent peaks. Assignment of resonances for organometallic complexes was made from

^{1}H–^{1}H COSY, ^{1}H–^{13}C HMQC and HMBC NMR experiments. Coupling constants are given in Hertz. Elemental analyses were performed by the Microanalytical Laboratory at the Institute of Chemistry of Rennes and are the average of two independent determinations.

^{13}C NMR analyses of polymers were performed in $CDCl_3$ solvent at 40 °C in either 5 mm or 10 mm tubes on AM-500 and AC-300 Bruker spectrometers operating at 125 and 75 MHz, respectively; "quantitative" ^{13}C NMR spectra were recorded in the inverted-gate decoupling-acquisition mode with the following parameters: delay 30 s, acquisition time 1.18 s, number of scans = 2000.

Spectral data for all diamagnetic complexes and polymer analytical data can be found in the Supporting Information.

GPC analyses of homo-sPS and sPS-PE copolymers were carried out in 1,3,6-trichlorobenzene at 135 °C in the Research Center of Total Petrochemicals in Feluy (Belgium) using PS standards for calibration. DSC measurements were performed on a TA Instruments DSC 2920 differential scanning calorimeter or a Mettler-Toledo DSC 822 apparatus, at a heating rate of 10 °C min^{-1}; first and second runs were recorded after cooling down to ca. 20 °C; the melting temperatures reported in Tables 3 and 4 correspond to second runs. DMA was carried out on a TA Instruments DMA 2980 apparatus, at a heating rate of 3 °C min^{-1} in the tension film mode with a deformation amplitude of 10 μm and 1 Hz frequency. TREF experiments were conducted at the Total-Arkema research center in Lacq, France, using solutions of polymers in xylene (0.3 g L^{-1}) prepared for 5 h at 130 °C. Solutions were typically injected at 130 °C in silica columns, cooled at 3 °C h^{-1} to 10 °C, and then eluted with xylene (1.0 mL min^{-1}) rising the temperature from 10 to 130 °C at 20 °C h^{-1}. A light-scattering evaporative detector DEDL 21 (Eurosep) was used. MALDI-TOF-MS was performed on a AutoFlex LT high-resolution spectrometer (Bruker Daltonics) which was operated in the reflector (19 kV) mode. The spectra were recorded in the positive-ion mode. The samples were prepared by taking 2 μL of a THF solution of the polymer (10 mg PS mL^{-1}) and adding this to 16 μL of 1,8-dihydroxy-9(10*H*)-anthracenone (dithranol, 10 mg mL^{-1} in THF) to which had been added 2 μL of CF_3SO_3Ag (2 mg mL^{-1} in THF). A 1 μL portion of this mixture was applied to the target and 50–100 single shot spectra were accumulated. Given masses represent the average masses of the Ag^+ adducts. The spectrometer was calibrated with an external mixture of angiotensin I, ACTH 18-39 and bovine insulin or PEG 1500.

[(Cp-CMe$_2$-Flu)Y(C$_3$H$_5$)(THF)] (2): A solution of allylmagnesium chloride (0.27 mL of a 2.0 M solution in THF, 0.54 mmol) was added to a suspension of **1** (0.390 g) in toluene (20 mL). The reaction mixture was stirred for 8 h at room temperature. The resulting yellowish-brown solution was filtered and volatiles were removed in vacuo. The residue was washed with pentane (2 × 15 mL) and dried in vacuo to give a yellow powder (0.16 g, 65 %). ^{1}H NMR ([D$_8$]toluene, 200 MHz, 25 °C): δ = 7.90 (d, 4H, $J_{H,H}$ = 8.4 Hz, Flu), 7.0–6.8 (m, 4H, Flu), 5.81 (t, 1H, $J_{H,H}$ = 2.6 Hz, Cp), 5.63 (q, 1H, $J_{H,H}$ = 12.2 Hz, CH_2CHCH_2), 5.57 (t, 1H, $J_{H,H}$ = 2.6 Hz, Cp), 2.94 (br m, 4H, α-CH_2, THF), 2.25 (s, 6H, CH_3), 1.72 (d, 4H, $J_{H,H}$ = 12.2 Hz, *anti*- and *syn*- CH_2CHCH_2), 1.13 ppm (br m, 4H, β-CH_2, THF); ^{13}C{^{1}H} NMR ([D$_8$]toluene, 75 MHz, 25 °C): δ = 144.5 (CH_2CHCH_2), 130.3 (quat. C, Cp), 125.3 (quat. C, Flu), 123.9 (Flu), 121.9 (Flu), 121.6 (Flu), 118.7 (quat. C, Flu), 117.1 (Flu), 109.6 (Cp), 99.2 (Cp), 93.8 (C-9, Flu), 72.5 (α-CH_2, THF), 68.8 (CH_2CHCH_2), 40.6 ($C(CH_3)_2$), 29.7 ($C(CH_3)_2$), 25.3 ppm (β-CH_2, THF); ^{1}H NMR ([D$_8$]toluene, 300 MHz, −70 °C): δ = 8.01 (d, 1H, $J_{H,H}$ = 7.9 Hz, Flu), 7.93 (d, 1H, $J_{H,H}$ = 7.9 Hz, Flu), 7.85 (d, 1H, $J_{H,H}$ = 7.9 Hz, Flu), 7.67 (d, 1H, $J_{H,H}$ = 7.9 Hz, Flu), 7.20–7.00 (m, 2H, overlapped with the signals from [D$_8$]toluene, Flu), 6.81 (t, 1H, $J_{H,H}$ = 7.9 Hz, Flu), 6.66 (t, 1H, $J_{H,H}$ = 7.9 Hz, Flu), 5.95 (s, 1H, Cp), 5.81 (s, 1H, Cp), 4.66 (m, 1H, overlapped with the signal from Cp, CH_2CHCH_2), 5.58 (s, 1H, Cp), 5.25 (s, 1H, Cp), 2.60 (br m, 4H, α-CH_2, THF), 2.60 (m, 1H, overlapped with the signal from THF, *syn*-CH_2CHCH_2), 2.33 (s, 3H, CH_3), 2.33 (m, 1H, overlapped with the signal from CH_3 group, *syn*-CH_2CHCH_2), 2.24 (s, 3H, CH_3), 1.66 (br m, 1H, *anti*-CH_2CHCH_2), 0.92 (br m, 4H, β-CH_2, THF), −0.43 ppm (br m, 1H, *anti*-CH_2CHCH_2); elemental analysis calcd (%) for $C_{28}H_{31}OY$: C 71.18, H 6.61; found: C 70.85, H 6.65.

[(Cp-CMe$_2$-Flu)La(C$_3$H$_5$)(THF)] (3): 2 equiv of *n*BuLi (2.54 mL of a 1.6 M solution in hexane, 4.07 mmol) were added under vigorous stirring to a solution of FluH-CMe$_2$-CpH (0.554 g, 2.03 mmol) in diethyl ether (50 mL) at −10 °C. The reaction mixture was allowed to warm to room temperature. The solution turned dark-yellow and over 3–4 h, a yellow crystalline powder precipitated. To this suspension of the dilithium salt in Et_2O cooled to −20 °C was added a suspension of [$LaCl_3(THF)_2$] (0.792 g, 2.03 mmol) in Et_2O (20 mL). Upon vigorous stirring and warming to room temperature, the reaction mixture turned pink. The solution was evaporated in vacuo to give a light pink powder. To the latter solid was added toluene (30 mL) and a solution of allylmagnesium chloride (1.02 mL of 2.0 M solution in THF, 2.04 mmol) was injected in by syringe. The reaction mixture was stirred for 8 h at room temperature. The resulting red-orange solution was filtered and volatiles were removed in vacuo. The residue was recrystallized from THF/toluene 1:1 mixture and dried in vacuo to give an orange powder (0.53 g, 50 %). Complex **3** was found to be sparingly soluble in toluene, and addition of THF was necessary to run NMR. ^{1}H NMR ([D$_8$]THF/[D$_8$]toluene (1:1), 200 MHz, 25 °C): δ = 8.01 (t, 4H, $J_{H,H}$ = 7.8 Hz, Flu), 7.2–6.8 (m, 4H, Flu), 6.12 (br m, 2H, Cp), 5.68 (br m, 2H, Cp), 5.26 (br m, 1H, CH_2CHCH_2), 2.24 (s, 6H, CH_3), 1.45 ppm (br m, 4H, CH_2CHCH_2); a ^{13}C NMR spectrum recorded under these conditions was not informative because significant decomposition of the complex took place due to the presence of THF; elemental analysis calcd (%) for $C_{28}H_{31}LaO$: C 64.37, H 5.98; found: C 64.05, H 5.00.

[(Cp-CMe$_2$-Flu)Nd(C$_3$H$_5$)(THF)] (4): Complex **4** was prepared from FluH-CMe$_2$-CpH (0.554 g, 2.03 mmol), [$NdCl_3(THF)_2$] (0.792 g, 2.03 mmol) and allylmagnesium chloride (1.02 mL of a 2.0 M solution in THF, 2.04 mmol) using a synthetic procedure similar as that described above for **2**, and isolated as a brown-green powder (0.920 g, 86 %). Elemental analysis calcd (%) for $C_{28}H_{31}NdO$: C 63.72, H 5.92; found: C 62.57, H 5.34.

[(Cp-CMe$_2$-Flu)Sm(C$_3$H$_5$)(THF)] (5): Complex **5** was prepared from FluH-CMe$_2$-CpH (0.607 g, 2.23 mmol), [$SmCl_3(THF)_2$] (0.893 g, 2.23 mmol) and allylmagnesium chloride (1.11 mL of a 2.0 M solution in THF, 2.23 mmol) using a synthetic procedure similar as that described above for **2**, and isolated as a brown powder (1.040 g, 87 %). Elemental analysis calcd (%) for $C_{28}H_{31}SmO$: C 62.99, H 5.85; found: C 62.00, H 5.38.

[(3-*t*Bu-Cp)-CMe$_2$-Flu)YCl(THF)] (6): 2 equiv of *n*BuLi (2.27 mL of a 1.6 M solution in hexane, 3.32 mmol) were added under vigorous stirring to a solution of (3-*t*Bu-CpH)-CMe$_2$-FluH (0.596 g, 1.814 mmol) in Et_2O (50 mL) at −10 °C. The reaction mixture was warmed to room temperature and the solution turned pink after 4 h. To this solution of the dilithium salt in Et_2O cooled to −20 °C was added a suspension of [$YCl_3(THF)_{3.5}$] (0.812 g, 1.81 mmol) in Et_2O (30 mL). Upon vigorous stirring and warming to room temperature, the reaction mixture turned bright-yellow. The solution was decanted, separated from the precipitate, and volatiles were removed in vacuo. The residue was recrystallized from benzene to give **6** as a bright-yellow microcrystalline powder (0.825 g, 87 %). ^{1}H NMR (200 MHz, [D$_8$]toluene, 25 °C) δ = 8.16 (m, 1H, Flu), 8.00–7.70 (m, 3H, Flu), 7.35–7.20 (m, 2H, Flu), 6.89 (t, 1H, $J_{H,H}$ = 7.4 Hz, Flu), 6.67 (t, 1H, $J_{H,H}$ = 7.4 Hz, Flu), 6.09 (br t, 1H, Cp), 5.57 (m, 2H, Cp), 3.08 (br m, 4H, α-CH_2, THF), 2.29 (s, 6H, CMe_2), 1.34 (s, 9H, *t*Bu), 1.08 ppm (br m, 4H, β-CH_2, THF); ^{13}C{^{1}H} NMR ([D$_8$]toluene, 75 MHz, 25 °C): δ = 142.1 (quat. C, Cp), 125.4 (quat. C, Cp; overlapped with signals from quat. C from Flu), 125.3 (overlapped with toluene resonances), 123.8, 122.3, 120.42, 119.6, 119.5, 119.3 (two signals overlapped), 117.0 (1,8-C, Flu), 106.8 (Cp), 102.2 (Cp), 101.7 (Cp), 93.3 (9-C, Flu), 71.3 (α-C, THF), 40.8 ($C(CH_3)_2$), 32.4 ($C(CH_3)_3$), 31.2 ($C(CH_3)_3$), 29.7 ($C(CH_3)$, CMe_2), 29.5 ($C(CH_3)$, CMe_2), 25.0 ppm (β-C, THF); elemental analysis calcd (%) for $C_{29}H_{34}ClOY$: C 66.61, H 6.55; found: C 66.01, H 6.87.

[(3-*t*Bu-Cp)-CMe$_2$-Flu)NdCl(THF)] (7): Complex **7** was prepared from FluH-CMe$_2$-(3-*t*Bu-CpH) (0.500 g, 1.52 mmol) and [$NdCl_3(THF)_2$] (0.600 g, 1.52 mmol) using a synthetic procedure similar as that described above for **6**, and isolated after recrystallization as a greenish-brown microcrystalline powder (0.598 g, 68 %). Elemental analysis calcd (%) for $C_{29}H_{34}ClNdO$: C 60.23, H 5.93; found: C 61.01, H 5.99.

[((3-*t*Bu-Cp)-CMe$_2$-Flu)Y(C$_3$H$_5$)(THF)] (8): A solution of allylmagnesium chloride (0.16 mL of a 2.0 M solution in THF, 0.320 mmol) was added to a solution of **6** (0.170 g, 0.325 mmol) in toluene (20 mL). The reaction mixture was stirred for 8 h at room temperature, the resulting orange solution was filtered and volatiles were removed in vacuo. The orange-yellow crystalline residue was recrystallized from toluene/hexane 2:1 to yield **8** (0.120 g, 69%). ^{1}H NMR (300 MHz, [D$_8$]toluene, 25°C): δ=8.02 (d, 1H, $J_{H,H}$=8.6 Hz, Flu), 7.95 (d, 1H, $J_{H,H}$=8.6 Hz, Flu), 7.79 (m, 2H, Flu), 7.15–6.85 (m, 4H with toluene signals, Flu), 6.20 (q, 1H, $J_{H,H}$= 12.2 Hz, CH$_2$C*H*CH$_2$), 5.82 (t, 1H, $J_{H,H}$=2.7 Hz, Cp), 5.73 (t, 1H, $J_{H,H}$= 2.7 Hz, Cp), 5.47 (t, 1H, $J_{H,H}$=2.7 Hz, Cp), 3.02 (br s, 4H, α-C*H*$_2$, THF), 2.20 (s, 3H, CMe$_2$), 2.17 (s, 3H, CMe$_2$), 1.83 (d, 4H, $J_{H,H}$=12.2 Hz, C*H*$_2$CHC*H*$_2$), 1.13 (br s, 4H, β-C*H*$_2$, THF), 1.09 ppm (s, 9H, CC*H*$_3$); ^{13}C{^{1}H} NMR ([D$_8$]toluene, 75 MHz, 25°C): δ=149.5 (CH$_2$*C*HCH$_2$), 139.1 (C-1, quat. C, Cp) 128.8 (Flu), 126.3 (quat. C, Flu), 125.5 (quat. C, Flu), 125.4 (C-3, quat. C, Cp), 125.2 (Flu), 122.4 (Flu), 122.1 (Flu), 120.5 and 120.4 (Flu), 119.8 and 119.6 (quat. C, Flu), 117.8 and 117.4 (Flu), 106.4 (Cp), 100.2 (Cp), 99.4 (Cp), 91.5 (C-9, Flu), 71.7 (α-*C*H$_2$, THF), 70.4 (*C*H$_2$CHCH$_2$), 40.5 (*C*Me$_2$), 31.9 (*C*(CH$_3$)$_3$), 31.6 (C(*C*H$_3$)$_3$), 29.6 (C-(*C*H$_3$)$_2$), 24.9 ppm (β-*C*H$_2$, THF); elemental analysis calcd (%) for C$_{32}$H$_{39}$Y: C 72.72, H 7.44; found: C 71.96, H 6.88.

[((3-*t*Bu-Cp)-CMe$_2$-Flu)Nd(C$_3$H$_5$)(THF)] (9): Complex **9** was prepared from **7** (0.300 g, 0.51 mmol) and allylmagnesium chloride (0.26 mL of a 2.0 M solution in THF, 0.51 mmol) using a synthetic procedure similar as that described above for **8**. The product was crystallized from toluene at room temperature to give green-violet crystals (0.163 g, 54%). Elemental analysis calcd (%) for C$_{32}$H$_{39}$NdO: C 65.82, H 6.73; found: C 66.12, H 6.98.

[(Cp-SiMe$_2$-Flu)Nd(μ-Cl)]$_2$ (11): 2 equiv of *n*BuLi (2.77 mL of a 2.5 M solution in hexane, 6.94 mmol) were added under vigorous stirring to a solution of CpH-SiMe$_2$-FluH (1.00 g, 3.47 mmol) in Et$_2$O (50 mL) at −30°C. The reaction mixture was warmed to room temperature and the solution turned pink after 4–5 h. To this solution of the dilithium salt in Et$_2$O cooled to −20°C was added a suspension of [NdCl$_3$(THF)$_2$] (1.370 g, 3.48 mmol) in Et$_2$O (30 mL). Upon vigorous stirring and warming to room temperature, the reaction mixture turned brown. This solution was decanted, separated from the precipitate, and volatiles were removed in vacuo. The residue was recrystallized from benzene at room temperature to give **11** as a greenish-brown microcrystalline powder (0.543 g, 46%).Elemental analysis calcd (%) for C$_{40}$H$_{36}$Cl$_2$Nd$_2$Si$_2$: C 51.53, H 3.89; found: C 52.3, H 4.23.

[(Cp-SiMe$_2$-Flu)Y(C$_3$H$_5$)(THF)] (12): A solution of allylmagnesium chloride (0.55 mL of a 2.0 M solution in THF, 1.094 mmol) was added to a solution of **10** (0.45 g, 0.547 mmol) in toluene (30 mL). The reaction mixture was stirred for 8 h at room temperature, the resulting yellow-orange solution was filtered and volatiles were removed in vacuo. The yellow solid obtained was recrystallized from toluene/hexane 1:1 to yield **12** (0.294 g, 55%) as yellow prisms. ^{1}H NMR ([D$_8$]toluene, 500 MHz, 25°C): δ=7.94 (d, 2H, $J_{H,H}$=8.4 Hz, Flu), 7.71 (d, 2H, $J_{H,H}$=8.4 Hz, Flu), 7.10 (t, 2H, $J_{H,H}$=8.4 Hz, Flu), 6.99 (t, 2H, $J_{H,H}$=8.4 Hz, Flu), 5.94 (s, 4H, Cp), 5.75 (q, 1H, $J_{H,H}$=12.1 Hz, CH$_2$C*H*CH$_2$), 2.97 (br m, 4H, α-C*H*$_2$, THF), 1.79 (d, 4H, $J_{H,H}$=12.1 Hz, *anti*- and *syn*- C*H*$_2$CHC*H*$_2$), 1.19 (br m, 4H, β-C*H*$_2$, THF), 0.99 ppm (s, 6H, C*H*$_3$); ^{13}C{^{1}H} NMR ([D$_6$]benzene, 125 MHz, 25°C): δ=146.7 (CH$_2$*C*HCH$_2$), 134.1 (quat. C, Flu), 128.1 (quat. C, Flu), 124.9 (Flu), 121.9 (Flu), 122.0 (Flu), 119.0 (Flu), 115.0 (Cp), 113.3 (quat. C, Cp), 110.5 (Cp), 75.7 (C-9, Flu), 71.8 (α-*C*H$_2$, THF), 69.5 (*C*H$_2$CHCH$_2$), 25.4 (β-*C*H$_2$, THF), −0.4 ppm (Si(*C*H$_3$)$_2$); ^{1}H NMR ([D$_8$]toluene, 500 MHz, −80°C): δ=8.08 (br s, 1H, Flu), 7.86 (br s, 1H, Flu), 7.78 (br s, 1H, Flu), 7.61 (br s, 1H, Flu), 7.33 (br m, 2H, Flu), 6.88 (br s, 1H, Flu), 6.77 (br s, 1H, Flu), 6.23 (s, 1H, Cp), 6.05 (s, 1H, Cp), 5.79 (m, 1H, overlapped with the signal from Cp, CH$_2$C*H*CH$_2$), 5.79 (s, 1H, Cp), 5.55 (s, 1H, Cp), 2.71 (m, 1H, *syn*-C*H*$_2$CHC*H*$_2$), 2.56 (br m, 4H, α-C*H*$_2$, THF), 2.25 (br s, 1H, *syn*-C*H*$_2$CHC*H*$_2$), 1.36 (m, 1H, *anti*-CH$_2$CHCH$_2$), 1.12 (br m, 4H, β-C*H*$_2$, THF), 1.04 (s, 3H, C*H*$_3$), 0.94 (s, 3H, C*H*$_3$), −0.43 ppm (br m, 1H, *anti*-C*H*$_2$CHC*H*$_2$); elemental analysis calcd (%) for C$_{27}$H$_{31}$OSiY: C 66.38, H 6.40; found: C 66.90, H 6.78.

[(Cp-SiMe$_2$-Flu)Nd(C$_3$H$_5$)(THF)] (13): Complex **13** was prepared from **11** (0.250 g, 0.268 mmol) and allylmagnesium chloride (0.27 mL of a 2.0 M solution in THF, 0.540 mmol) using a synthetic procedure similar as that described above for **12**. The product was recrystallized from benzene at room temperature to give a greenish crystalline solid (0.186 g, 64%). Elemental analysis calcd (%) for C$_{27}$H$_{31}$OSiNd: C 59.63, H 5.75; found: C 60.10, H 5.25.

Solid-state structure determination of complexes 4, 9 and 12: Suitable single crystals were mounted onto a glass fiber using the "oil-drop" method. Diffraction data were collected at 100 K using either a NONIUS Kappa CCD or an APEX Bruker diffractometer with graphite monochromatized Mo$_{K\alpha}$ radiation (λ=0.71073 Å). A combination of ω- and ϕ scans was carried out to obtain at least a unique data set. Crystal structures were solved by means of the Patterson method, remaining atoms were located from difference Fourier synthesis, followed by full-matrix least-squares refinement based on F^2 (programs SHELXS-97 and SHELXL-97).[67] Many hydrogen atoms could be found from the Fourier Difference. Carbon-bound hydrogen atoms were placed at calculated positions and forced to ride on the attached carbon atom. The hydrogen atom contributions were calculated but not refined. All non-hydrogen atoms were refined with anisotropic displacement parameters. The locations of the largest peaks in the final difference Fourier map calculation as well as the magnitude of the residual electron densities were of no chemical significance.

Crystal data for **4**: C$_{28}$H$_{31}$NdO, M=527.77, orthorhombic, a=28.9132(7), b=7.8898(2), c=9.5349(2) Å, α=90, β=90, γ=90°, V=2175.10(9) Å^3, T=100(2) K, space group *Pna*2$_1$ (no. 33), Z=4, ρ_{calcd}=1.612 g cm^{-3}, crystal size=0.14×0.11×0.06 mm^3, μ(Mo$_{K\alpha}$)=2.404 mm^{-1}, 15543 reflections measured, 4710 unique and 3623 reflections with $I>2\sigma(I)$ which were used in all calculations. The final $R1$ was 0.0503 (observed data) and $wR2$ was 0.1362 (all data).

Crystal data for **9**: C$_{32}$H$_{39}$NdO, M=583.87, tetragonal, a=33.0860(4), b= 33.0860(4), c=10.044(4) Å, α=90, β=90°, γ=90°, V=10994.78(19) Å^3, T=100(2) K, space group $I4_1/a$ (no. 88), Z=16, ρ_{calcd}=1.411 g cm^{-3}, crystal size=0.07×0.06×0.05 mm^3, μ(Mo$_{K\alpha}$)=1.910 mm^{-1}, 107253 reflections measured, 6442 unique and 5549 reflections with $I>2\sigma(I)$ which were used in all calculations. The final $R1$ was 0.0464 (observed data) and $wR2$ was 0.1535 (all data). The unit cell of complex **9** contains a disordered solvent molecule that was not refined.

Crystal data for **12**: C$_{27}$H$_{31}$OSiY, M=488.52, orthorhombic, a=7.9908(3), b=16.6565(8), c=16.9749(8) Å, α=90, β=90, γ=90°, V= 2259.34(17) Å^3, T=100(2) K, space group P_{212121} (no. 19), Z=4, ρ_{calcd}= 1.436 g cm^{-3}, crystal size=0.55×0.25×0.20 mm3, μ(Mo$_{K\alpha}$)=2.651 mm^{-1}, 36762 reflections measured, 5051 unique and 4731 reflections with $I>2\sigma(I)$ which were used in all calculations. The final $R1$ was 0.0221 (observed data) and $wR2$ was 0.0560 (all data).

CCDC-253184 (**4**), -629127 (**9**) and -629128 (**12**) contain the supplementary crystallographic data for this paper. These data can be obtained free of charge from The Cambridge Crystallographic Data Centre via www.ccdc.cam.ac.uk/data_request/cif.

Typical procedure for styrene polymerization: In the glovebox, a preweighed amount of allyl *ansa*-lanthanidocene (ca. 15 mg) was added to styrene (3.00 mL, 26.0 mmol) and vigorous stirring at the appropriate temperature was immediately started. After a given time period, the Schlenk tube was opened to air and a 10% solution of HCl in methanol (ca. 1 mL) was added to quench the reaction. The precipitated polymer was washed repeatedly with methanol (ca. 500 mL), filtered and dried in vacuo overnight at room temperature.

Typical procedure for styrene–ethylene copolymerization: A 300 mL glass high-pressure reactor was charged with 50 mL of freshly distilled solvent (if needed) under argon flash. The reactor was then purged with ethylene and loaded with styrene at atmospheric pressure, and then kept at the desired temperature by circulating water in a double wall. A solution of catalyst in 2 mL of toluene was injected in by syringe. Mechanical stirring (Pelton turbine, 1000 rpm) was started immediately and the gas pressure in the reactor was maintained constant with a back regulator throughout the experiment. The ethylene consumption was monitored via an Aalborg flowmeter. After a given time period, the reactor was depressurized and the reaction was quenched by adding ca. 5 mL of a 10% solution of HCl in methanol. The polymer was further precipitated

by adding 500 mL of methanol, washed and dried in vacuo overnight at room temperature.

The fraction of styrene in the copolymer F_{sty} was determined using the equation:

$$F_{sty} = \frac{4A_{Ph}}{A_{Ph} + 5A_{Me}}$$

where A_{Ph} is the area of the aromatic styrene proton resonances (δ 7.5–6.2 ppm) and A_{Me} is the area of methylene and methine proton resonances of styrene and ethylene (δ 1.2–2.1 ppm) in the ^{1}H NMR spectrum.

Acknowledgements

We gratefully thank Total Co. for supporting this research (post-doctoral fellowship to E.K. and Ph.D. grant to A.S.R.). We are most grateful to Mr. V. Bellia (Total Petrochemicals) for technical support, Dr. C. Lamotte (Total Petrochemicals), Dr. C. Degoulet (Total Arkema) and Dr. A. Bourmaud (Univ. of Lorient) for analysis of some polymers by NMR, TREF and DMA techniques, respectively, and Professor V. Busico (Univ. of Napoli) for advice on microstructural analysis of polymers by NMR techniques.

[1] a) H. H. Brintzinger, D. Fischer, R. Mülhaupt, B. Rieger, R. M. Waymouth, *Angew. Chem.* **1995**, *107*, 1255; *Angew. Chem. Int. Ed. Engl.* **1995**, *34*, 1143; b) A. Zambelli, P. Ammendola, *Prog. Polym. Sci.* **1991**, *16*, 203; c) J. A. Gladysz, *Chem. Rev.* **2000**, *100*, 1167.

[2] For the book chapters and reviews on the synthesis of syndiotactic polystyrene see: a) K. Yokota, T. Inoue, H. Shozaki, N. Tomotsu, M. Kuramoto, N. Ishihara in *Metalorganic Catalysts for Synthesis and Polymerization*, Springer, Heidelberg, **1999**, p. 435; b) N. Ishihara in *Progress and Development of Catalytic Olefin Polymerization*, Technology and Education Publishers, Tokyo, **2000**, p. 121; c) "Synthesis of syndiotactic polystyrene": N. Tomotsu, M. Malanga, J. Schellenberg in *Modern Styrenic Polymers: Polystyrenes and Styrenic Copolymers*, Wiley, Chichester, **2003**, p. 365; d) R. Po, N. Cardi, *Prog. Polym. Sci.* **1996**, *21*, 47; e) N. Tomotsu, N. Ishihara, T. H. Newman, M. T. Malanga, *J. Mol. Catal. A* **1998**, *128*, 167; f) J. Schellenberg, N. Tomotsu, *Prog. Polym. Sci.* **2002**, *27*, 1925.

[3] N. Ishihara, T. Seimiya, M. Kuramoto, M. Uoi, *Macromolecules* **1986**, *19*, 2464.

[4] For examples of half-titanocene catalysts for the production of sPS see: a) N. Ishihara, M. Kuramoto, M. Uoi, *Macromolecules* **1988**, *21*, 3356; b) C. Pellecchia, D. Pappalardo, L. Oliva, A. Zambelli, *J. Am. Chem. Soc.* **1995**, *117*, 6593; c) Q. Wang, R. Quyoum, D. J. Gillis, M.-J. Tudoret, D. Jeremic, B. K. Hunter, M. C. Baird, *Organometallics* **1996**, *15*, 693; d) S. Y. Knjazhanski, G. Cadenas, M. Garcia, C. M. Perez, I. E. Nifant'ev, I. A. Kashulin, P. V. Ivchenko, K. Lyssenko, *Organometallics* **2002**, *21*, 3094.

[5] a) J. C. Flores, J. C. W. Chien, M. D. Rausch, *Organometallics* **1995**, *14*, 1927; b) J. C. Flores, J. C. W. Chien, M. D. Rausch, *Organometallics* **1995**, *14*, 2106.

[6] a) D. Liguori, F. Grisi, I. Sessa, A. Zambelli, *Macromol. Chem. Phys.* **2003**, *204*, 164; b) D. Liguori, R. Centore, A. Tuzi, F. Grisi, I. Sessa, A. Zambelli, *Macromolecules* **2003**, *36*, 5451.

[7] a) J. Okuda, E. Masoud, *Macromol. Chem. Phys.* **1998**, *199*, 543; b) C. Capacchione, A. Proto, H. Ebeling, R. Mülhaupt, K. Moller, T. P. Spaniol, J. Okuda, *J. Am. Chem. Soc.* **2003**, *125*, 4964; c) C. Capacchione, A. Proto, H. Ebeling, R. Mülhaupt, K. Moller, R. Manivannan, T. P. Spaniol, J. Okuda, *J. Mol. Catal. A* **2004**, *213*, 137.

[8] Y. Luo, J. Baldamus, Z. Hou, *J. Am. Chem. Soc.* **2004**, *126*, 13910.

[9] J. Hitzbleck, K. Beckerle, J. Okuda, R. Mülhaupt, *Macromol. Symp.* **2006**, *236*, 23.

[10] For the INSITE technology from Dow Co., see: a) S. Bensanson, J. Minick, S. P. Chum, A. Hiltner, E. Baer, *J. Polym. Sci. Part B* **1996**, *34*, 1301; b) H. Y. Chen, M. J. Guest, S. P. Chum, A. Hiltner, E. Baer, *J. Appl. Polym. Sci.* **1998**, *70*, 109; c) H. Y. Chen, E. V. Stepanov, S. P. Chum, A. Hiltner, E. Baer, *J. Polym. Sci. Part B* **1999**, *37*, 2372; d) H. Y. Chen, E. V. Stepanov, S. P. Chum, A. Hiltner, E. Baer, *Macromolecules* **1999**, *32*, 7587; e) P. S. Chum, W. J. Kruper, M. J. Guest, *Adv. Mater.* **2000**, *12*, 1759; f) J. C. Stevens, F. J. Timmers, D. R. Wilson, G. F. Schmidt, P. N. Nickias, R. K. Rosen, G. W. Knight, S. Lais, The Dow Chemical Company, US Pat. Appl. 5703187; Eur. Pat. Appl. 416815A1, **1991**.

[11] For some early pioneering works on the preparation of ethylene–styrene copolymers with low styrene incorporation (0.1–20 mol%), see: a) T. Mityatake, K. Mizunuma, M. Kakugo, *Makromol. Chem. Macromol. Symp.* **1993**, *66*, 203; b) R. Mani, C. M. Burns, *Macromolecules* **1991**, *24*, 5476; c) P. Aaltonen, J. Seppala, L. Matilainen, M. Leskela, *Macromolecules* **1994**, *27*, 3136; d) J. Ren, G. R. Hatfield, *Macromolecules* **1995**, *28*, 2588; e) H. F. Richards, W. Greek, Shell Oil Co. US Pat. Appl. 3390141, **1968**.

[12] For recent examples on the preparation of ethylene–styrene copolymers see: a) L. Oliva, L. Caporaso, C. Pellecchia, A. Zambelli, *Macromolecules* **1995**, *28*, 4665; b) C. Pellecchia, D. Pappalardo, M. D'Arco, A. Zambelli, *Macromolecules* **1996**, *29*, 1158; c) S. Fokken, T. P. Spaniol, J. Okuda, F. G. Sernetz, R. Mülhaupt, *Organometallics* **1997**, *16*, 4240; d) G. Xu, S. Lin, *Macromolecules* **1997**, *30*, 685; e) G. Xu, *Macromolecules* **1998**, *31*, 2395; f) K. Nomura, H. Okumura, T. Komatsu, N. Naga, *Macromolecules* **2002**, *35*, 5388; g) K. Nomura, H. Okumura, T. Komatsu, N. Naga, Y. Imanishi, *J. Mol. Catal. A* **2002**, *190*, 225; h) I. Albers, W. Kaminsky, U. Weingarten, W. Werner, *Catal. Commun.* **2002**, *3*, 105; i) R. Skeril, P. Sindelar, Z. Salajka, V. Varga, I. Cisarova, J. Pinkas, M. Horacek, K. Mach, *J. Mol. Catal. A* **2004**, *224*, 97; j) Q. Wang, P. Lam, G. T. Yamashita, Nova Chemicals S.A. , US Patent 6806329B2, **2004**.

[13] N. Guo, T. J. Marks, *J. Am. Chem. Soc.* **2004**, *126*, 6542.

[14] a) H. Zhang, K. Nomura, *J. Am. Chem. Soc.* **2005**, *127*, 9364; b) H. Zhang, K. Nomura, *Macromolecules* **2006**, *39*, 5266.

[15] Preliminary communications: a) E. Kirillov, C. W. Lehmann, A. Razavi, J.-F. Carpentier, *J. Am. Chem. Soc.* **2004**, *126*, 12240; b) J.-F. Carpentier, E. Kirillov, A. Razavi, A.-S. Rodrigues, Univ. Rennes 1 and Total Petrochemicals Research, Eur. Pat. Appl. 04/290847, PCT Int. Appl. 2005/051369; WO 2005/095470; c) A.-S. Rodrigues, E. Kirillov, J.-F. Carpentier, *Intern. Conf. on Organomet. Chem. (ICOMC XXII)*, Zaragoza (Spain), 23–28 July **2006**.

[16] M. Tsutsui, N. Ely, *J. Am. Chem. Soc.* **1975**, *97*, 3551.

[17] G. Jeske, H. Lauke, H. Mauermann, P. N. Swepston, H. Schumann, T. J. Marks, *J. Am. Chem. Soc.* **1985**, *107*, 8091.

[18] a) W. J. Evans, T. A. Ulibarri, J. W. Ziller, *J. Am. Chem. Soc.* **1990**, *112*, 2314; b) W. J. Evans, D. M. DeCoster, J. Greaves, *Organometallics* **1996**, *15*, 3210; c) W. J. Evans, S. A. Kozimor, J. C. Brady, B. L. Davis, G. W. Nyce, C. A. Seibel, J. W. Ziller, R. J. Doedens, *Organometallics* **2005**, *24*, 2269.

[19] a) J. C. Yoder, M. W. Day, J. E. Bercaw, *Organometallics* **1998**, *17*, 4946; b) M. B. Abrams, J. C. Poder, C. Loeber, M. W. Day, J. E. Bercaw, *Organometallics* **1999**, *18*, 1389.

[20] a) T. J. Woodman, M. Schormann, D. L. Hughes, M. Bochmann, *Organometallics* **2003**, *22*, 3028; b) T. J. Woodman, M. Schormann, M. Bochmann, *Organometallics* **2003**, *22*, 2938; c) T. J. Woodman, M. Schormann, D. L. Hughes, M. Bochmann, *Organometallics* **2004**, *23*, 2972; d) L. F. Sanchez-Barba, D. L. Hughes, S. M. Humphrey, M. Bochmann, *Organometallics* **2005**, *24*, 3792.

[21] a) M. Brunelli, S. Poggio, U. Pedretti, G. Lugli, *Inorg. Chim. Acta* **1987**, *131*, 281; b) R. Taube, S. Mainwald, J. Sieler, *J. Organomet. Chem.* **1996**, *513*, 37; c) R. Taube, S. Mainwald, J. Sieler, *J. Organomet. Chem.* **2001**, *621*, 327; d) C. P. Casey, J. A. Tunge, M. Fagan, *J. Organomet. Chem.* **2002**, *663*, 91; e) C. J. Kuehl, C. K. Simpson, K. D. John, A. P. Sattelberger, C. N. Carlson, T. P. Hanusa, *J. Organomet. Chem.* **2003**, *683*, 149.

[22] a) For ethylene and α-olefins polymerization using base-free allyl bis(cyclopentadienyl) complexes of samarium and yttrium, see reference [18]; b) styrene polymerization giving stereotactic-enriched materials (r or $m < 80\%$): D. Baudry-Barbier, E. Camus, A. Dormond,

M. Visseaux, *Appl. Organomet. Chem.* **1999**, *13*, 813; c) Stereospecific (up to 97% of *trans*-1,4) isoprene polymerization: D. Baudry-Barbier, N. Andre, A. Dormond, C. Pardes, P. Richard, M. Visseaux, C.-J. Zhu, *Eur. J. Inorg. Chem.* **1998**, 1721; d) for butadiene polymerization, see reference [21c]; e) for ROP of *rac*-lactide and ε-caprolactone, see reference [20d].

[23] E. Kirillov, L. Toupet, C. W. Lehmann, A. Razavi, S. Kahlal, J.-Y. Saillard, J.-F. Carpentier, *Organometallics* **2003**, *22*, 4038.

[24] E. Kirillov, C. W. Lehmann, A. Razavi, J.-F. Carpentier, *Organometallics* **2004**, *23*, 2768.

[25] The reaction of **1** with the methyl-substituted Grignard reagent ClMg(2-Me-C_3H_4) yields a yellow microcrystalline material, of which the elemental analysis is consistent with the expected formula [(Flu-CMe_2-Cp)Y(2-Me-C_3H_4)(THF)]. However, this product was surprisingly found to be virtually insoluble in common organic solvents (pentane, toluene, diethyl ether, THF), which merely hampered its formal authentication.

[26] a) H. Schumann, J. A. Meese-Marktscheffel, L. Esser, *Chem. Rev.* **1995**, *95*, 865; b) R. Anwander, *Top. Organomet. Chem.* **1999**, *2*, 1; c) in addition to the aforementioned examples, *ansa*-samarocene [{Me_2Si(3-Me_3Si-C_5H_2)$_2$}Sm(CH($SiMe_3$)$_2$)(THF)] constitutes a rare example of a mono-THF adduct: G. Desurmont, Y. Li, H. Yasuda, T. Maruo, N. Kanehisa, Y. Kai, *Organometallics* **2000**, *19*, 1811.

[27] a) E. Kirillov, J.-Y. Saillard, J.-F. Carpentier, *Coord. Chem. Rev.* **2005**, *249*, 1221; b) B. Wang, *Coord. Chem. Rev.* **2006**, *250*, 242; c) J. Gromada, J.-F. Carpentier, A. Mortreux, *Coord. Chem. Rev.* **2004**, *248*, 397; d) P. J. Shapiro, *Coord. Chem. Rev.* **2002**, *231*, 67; e) J. C. Green, *Chem. Soc. Rev.* **1998**, *27*, 263.

[28] a) C. Qian, W. Nie, J. Sun, *Organometallics* **2000**, *19*, 4134; b) W. Nie, C. Qian, Y. Chen, J. Sun, *J. Organomet. Chem.* **2002**, *647*, 114.

[29] However, upon heating at 80°C over 12 h, significant decomposition to unidentified materials was observed by ^{1}H NMR spectroscopy.

[30] Crystals of **2** were obtained upon recrystallization of the crude material from toluene at 80°C and analyzed by X-ray diffraction. Usual data refinement enabled to confirm the atom connectivity in **2**. However, the poor *R* factor value does not allow discussing geometrical parameters (bond lengths and angles).

[31] The unit cells of both **4** and **12** contain two racemic pairs ($Z=4$) of homochiral molecules, that is, *R* and *S* isomers, respectively. Taking into account the C_1-symmetrical environment in tetrahedral complex **12**, two diastereomeric racemic pairs might form. However, only one diastereomerically pure racemic pair of molecules, in which the THF and *t*Bu-group are *trans*-positioned with respect to each other, was found eight times translated ($Z=16$) in the unit cell of **12**.

[32] a) C. Qian, W. Nie, J. Sun, *J. Chem. Soc. Dalton Trans.* **1999**, 3283; b) C. Qian, W. Nie, J. Sun, *J. Organomet. Chem.* **2001**, *626*, 171.

[33] M. H. Lee, J.-W. Hwang, J. Kim, Y. Han, Y. Do, *Organometallics* **1999**, *18*, 5124.

[34] The allyl ligand in **12** is disordered with the methine carbon directed up and down in the crystal lattice.

[35] Lanthanum allyl complex **3** appeared to be unstable in mixed [D_8]THF/[D_8]toluene solution (see Experimental Section), which hampered its characterization by NMR techniques.

[36] The ^{1}H NMR spectra of neodymium and samarium allyl complexes **4**, **5**, **9** and **13** displayed broad resonances due to the strong paramagnetic properties of the metal centers and were uninformative.

[37] For recent references on the fluxional behavior of allyl group in transition metal complexes see: a) ref. [19] and references therein; b) ref. [18]; c) C. N. Carlson, T. P. Hanusa, W. W. Brennessel, *J. Am. Chem. Soc.* **2004**, *126*, 10550; d) L. C. Silva, P. T. Gomes, L. F. Veiros, S. I. Pascu, M. T. Duarte, S. Namorado, J. Ascenso, A. R. Dias, *Organometallics* **2006**, *25*, 4391.

[38] For references on the fluxional behavior of mono-THF adducts of lanthanide complexes, see ref. [24] and references therein.

[39] a) P. M. Treichel, J. W. Johnson, *Inorg. Chem.* **1977**, *16*, 749; b) A. Albright, P. Hofmann, R. Hoffmann, C. P. Lillya, P. A. Dobosh, *J. Am. Chem. Soc.* **1983**, *105*, 3396; c) Y. F. Oprunenko, *Russ. Chem. Rev.* **2000**, *69*, 683.

[40] Base-mediated inter-ring haptotropic rearrangements in bis-(indenyl)zirconium complexes have been reported very recently: a) C. A. Bradley, E. Lobkovski, I. Keresztes, P. K. Chirik, *J. Am. Chem. Soc.* **2005**, *127*, 10291; b) L. F. Veiros, *Organometallics* **2006**, *25*, 2266.

[41] M. Bochmann, S. J. Lancaster, M. B. Hursthouse, M. Mazid, *Organometallics* **1993**, *12*, 4718.

[42] E. Kirillov, L. Toupet, C. W. Lehmann, A. Razavi, J.-F. Carpentier, *Organometallics* **2003**, *22*, 4467.

[43] D. Drago, P. S. Pregosin, A. Razavi, *Organometallics* **2000**, *19*, 1802.

[44] C. Pellecchia, A. Proto, A. Zambelli, *Macromolecules* **1992**, *25*, 4450.

[45] Effective ionic radii for eight-coordinate metal centers: La^{3+}: 1.160 Å, Nd^{3+}: 1.109 Å, Sm^{3+}: 1.079 Å, Y^{3+}: 1.019 Å; R. D. Shannon, *Acta Crystallogr. Sect. A* **1976**, *32*, 751.

[46] Complex **3** is unstable in solution, even at room temperature. See the Experimental Section for details.

[47] F. R. Mayo, *J. Am. Chem. Soc.* **1968**, *90*, 1289.

[48] Syndiotactic polystyrene exhibits a complex polymorphic behavior in the solid state. Four crystalline forms of sPS, known as α, β, γ and δ, have been reported, which feature each different melting points in the range 250–273°C, according to the molecular weight, see: G. Guerra, M. Vitagliano, C. De Rosa, V. Petraccone, P. Corradini, *Macromolecules* **1990**, *23*, 1539.

[49] Nevertheless, several fractionation tests were conducted to prove the homogeneity of the PE-PS samples. Thus, Soxhlet separation (chloroform/hexane 5:1 or neat THF) gave only one solid phase in all cases.

[50] No evidence of styrene misinsertions, that is, regioirregular head-to-head and tail-to-tail sequences, was observed.

[51] At this stage, we can not assign those minor resonances. They may correspond either to terminal styrene units in "pure" syndiotactic polystyrene sequences, having a different magnetic environment due to the close vicinity of ethylene units, or to atactic polystyrene sequences.

[52] Q. Wang, P. Lam, Z. Zhang, G. Yamashita, L. Fan, US Pat 6579961B1, **2002** (to Nova Chem.).

[53] A. Grassi, S. Saccheo, A. Zambelli, F. Laschi, *Macromolecules* **1998**, *31*, 5588.

[54] a) T. E. Ready, R. Gurge, J. C. W. Chien, M. D. Rausch, *Organometallics* **1998**, *17*, 5236; b) M. Mahanthappa, R. M. Waymouth, *J. Am. Chem. Soc.* **2001**, *123*, 12093.

[55] Complex **14** can also be activated for syndiotactic styrene polymerization using an excess of a dialkyl- or diallyl–magnesium reagent, allowing effective reversible transfer to the latter Grignard reagent: a) A.-S. Rodrigues, E. Kirillov, A. Razavi, J.-F. Carpentier, unpublished results; for binary lanthanide–dialkylmagnesium polymerization systems and their use in styrene polymerization, see: b) X. Olonde, A. Mortreux, F. Petit, K. Bujadoux, *J. Mol. Catal.* **1993**, *82*, 75; c) J.-F. Pelletier, A. Mortreux, X. Olonde, K. Bujadoux, *Angew. Chem.* **1996**, *108*, 1980; *Angew. Chem. Int. Ed. Engl.* **1996**, *35*, 1854; d) S. Bogaert, J.-F. Carpentier, T. Chenal, A. Mortreux, G. Ricart, *Macromol. Chem. Phys.* **2000**, *201*, 1813; e) S. Bogaert, T. Chenal, A. Mortreux, G. Nowogrocki, C. W. Lehmann, J.-F. Carpentier, *Organometallics* **2001**, *20*, 199; f) Y. Sarazin, T. Chenal, A. Mortreux, H. Vezin, J.-F. Carpentier, *J. Mol. Catal. A* **2005**, *238*, 207.

[56] Note, however, that it was not possible to distinguish unambiguously between a CH_2=CH-CH_2-CHPh or CH_2=CH-(CH_2)$_2$-CHPh group, and thus to assess the regioselectivity (1,2- or 2,1-insertion mode) of the first insertion of styrene.

[57] a) C. Pellecchia, P. Longo, A. Grassi, P. Ammendola, A. Zambelli, *Makromol. Chem. Rapid Commun.* **1987**, *8*, 277; b) A. Zambelli, P. Lango, C. Pallecchia, A. Grassi, *Macromolecules* **1987**, *20*, 2037.

[58] F. Feil, S. Harder, *Macromolecules* **2003**, *36*, 3446.

[59] Distribution of the syndiotactic stereosequences at the heptad level using chain-end model were calculated from the following equations: $rrrrrr = (1-P_m)^6$, *rrmrrr*, *rmrrrr* and $mrrrrr = 2P_m(1-P_m)^5$; see: V. Busico, R. Cipullo, *Prog. Polym. Sci.* **2001**, *26*, 443. The calculated values are 0.74, 0.08, 0.08 and 0.08, respectively.

[60] The following equations were used: $rrrr = (1-P_m)^4$, *rrmr* and *mrrr* $= 2P_m(1-P_m)^3$, see ref. [59]. The calculated values are 0.82, 0.084 and 0.084, respectively, and the experimental values are 0.82, 0.09 and 0.09, respectively.
[61] However, the syndiotacticity of the polystyrenes prepared using complexes **8** and **9** at room temperature is somewhat lower than that of polystyrenes prepared under the same conditions with complex **4**. The ^{13}C NMR spectrum of the former polystyrenes is similar to that of a polystyrene prepared at 120 °C with **4** (see Figure 15).
[62] In the polymerization of α-olefins catalyzed by Group 4 metallocenes the C_1-symmetry precursors produce highly isotactic polymers via enantiomorphic site control mechanism. See: a) A. Razavi, V. Bellia, Y. De Brauwer, K. Hortmann, L. Peters, S. Sirol, S. Van Belle, U. Thewalt, *Macromol. Chem. Phys.* **2004**, *205*, 347; b) A. Razavi, U. Thewalt, *Coord. Chem. Rev.* **2006**, *250*, 155, and references therein.
[63] a) G. Minieri, P. Corradini, A. Zambelli, G. Guerra, L. Cavallo, *Macromolecules* **2001**, *34*, 2459; b) G. Minieri, P. Corradini, G. Guerra, A. Zambelli, L. Cavallo, *Macromolecules* **2001**, *34*, 5379.
[64] a) S. H. Yang, J. Huh, J. S. Yang, W. H. Jo, *Macromolecules* **2004**, *37*, 5741; b) S. H. Yang, J. Huh, W. H. Jo, *Organometallics* **2006**, *25*, 1144.
[65] It should be emphasized again that primary insertion is strictly unfavorable due to the strong repulsive interaction between two phenyl groups of the pre-inserted styrene and the next approaching styrene molecules.
[66] For computational works on ethylene–styrene copolymerization using model geometries like CpTi, [CGC]Ti and *rac*-$(CH_2)_2(Ind)_2M$ (M = Ti, Zr), see: a) A. Munoz-Escalona, V. Cruz, N. Mena, S. Martinez, J. Martinez-Salazar, *Polymer* **2002**, *43*, 7017; b) S. Martinez, V. Cruz, A. Munoz-Escalona, J. Martinez-Salazar, *Polymer* **2003**, *44*, 295; c) S. H. Yang, W. H. Jo, S. K. Noh, *J. Chem. Phys.* **2003**, *119*, 1824; d) M. T. Exposito, S. Martinez, J. Ramos, V. Cruz, M. Lopez, A. Munoz-Escalona, N. Haider, J. Martinez-Salazar, *Polymer* **2004**, *45*, 9029; e) J. Ramos, A. Munoz-Escalona, S. Martinez, J. Martinez-Salazar, *J. Chem. Phys.* **2005**, *122*, 74901; f) S. Martinez, M. T. Exposito, J. Ramos, V. Cruz, M. C. Martinez, M. Lopez, A. Munoz-Escalona, J. Martinez-Salazar, *J. Polym. Sci. Part A* **2005**, *43*, 711.
[67] a) G. M. Sheldrick, SHELXS-97, Program for the Determination of Crystal Structures, University of Goettingen, Germany, **1997**; b) G. M. Sheldrick, SHELXL-97, Program for the Refinement of Crystal Structures, University of Goettingen, Germany, **1997**.

Received: November 29, 2006
Published online: February 19, 2007

